Glial Na_x channels control lactate signaling to neurons for brain $[Na^+]$ sensing

by

Hidetada Shimizu

DOCTOR OF PHILOSOPHY

in

Department of Basic Biology

School of Life Science

The Graduate University for Advanced Studies

2007

Abstract

Sodium (Na) homeostasis is crucial for life and Na levels in body fluids are constantly monitored in the brain. The subfornical organ (SFO) is the center of the sensing responsible for the control of Na-intake behavior, where Na_x channels are expressed in specific glial cells as the Na-level sensor. Na_x channel is a concentration-sensitive Na channel with a threshold value of approximately 150 mM for the extracellular Na ion. The Na_x-positive glial cells are sensitive to an increase in the extracellular Na level in the physiological range, indicating that glial cells, not neurons, are the primary site of Na-level sensing. However, the mechanism by which the Na signal sensed by "inexcitable" glial cells is transferred to neurons has remained to be elucidated.

To gain insight into the cellular processes involving Na_x in glial cells, in this doctor thesis, I started in my study with screening for molecules interacting with Na_x using the yeast two-hybrid system with each of the cytoplasmic domains of mouse Na_x as bait. Among the positive clones isolated from a mouse DRG cDNA library by using the C-terminal region of Na_x as bait, three clones coded for the α subunit of Na^+/K^+-ATPase. A detailed analysis revealed that all these clones were identical and coded amino acid sequence of the region close to the cytoplasmic catalytic domain of the α1 subunit of Na^+/K^+-ATPase. The direct interaction between Na_x and the α1 subunit of Na^+/K^+-ATPase was verified by pull-down assays and the immunoprecipitation of the cell lysate.

Coexpression of the α1 subunit of Na^+/K^+-ATPase and Na_x channels was examined by double-fluorescent immunostaining using sections of the SFO and dissociated cells from the SFO. The α1 subunit was broadly distributed throughout the

SFO, overlapping with the expression of Na_x channels. The confocal microscopic analyses with isolated cells from the SFO showed that both molecules were colocalized in the plasma membrane. Na_x channels were expressed in large round cells, but not in small cells with neurite-like processes, indicating that Na_x channels are expressed in glial cells including ependymal cells.

It is known that the α2 and α3 isoforms of Na^+/K^+-ATPase are also expressed in the brain. Experiments using the yeast two-hybrid system showed that the cytoplasmic fragment of α2 corresponding to the region of the α1 isoform isolated also interacted with the C-terminal region of Na_x, but that of α3 did not. Thus, Na_x has specific interaction with α1 and α2 isoforms of Na^+/K^+-ATPase. By *in situ* hybridization, I verified that the mRNAs encoding the α1 and α2 isoforms of Na^+/K^+-ATPase were expressed in the SFO with a similar pattern to the Na_x channels. However, signals for the α3 isoform were not detected in the SFO.

I speculated that Na_x may functionally regulate Na^+/K^+-ATPase through the close interaction between the two. To examine this idea *in vitro*, I established cell lines using C6 glioma cells in which the expression of Na_x channel is inducible under a tetracycline-based system. I preferentially used one of the cell lines thus prepared, C6M16, for the following experiments. C6M16 cells showed significant Na^+ influx in response to an increase in the extracellular Na level within the physiological range (from 145 mM to 170 mM) specifically under the conditions where Na_x channels are expressed.

If the molecular properties of the Na^+/K^+-ATPase is changed by Na_x, cellular metabolism should be affected accordingly, because cells in the CNS use ~50% of their energy resources to drive the Na^+/K^+-ATPase activity. I then compared the cellular

uptakes of a fluorescent glucose derivative (2-NBDG) in isotonic (145 mM) and hypertonic (170 mM) Na solutions. The C6M16 cells with Na_x expression showed approximately 1.6-fold greater activity for 2-NBDG uptake in the 170 mM Na solution as compared with in the 145 mM solution, while the uptake by the C6M16 cells without Na_x expression was not increased in the 170 mM Na solution. The increase in the uptake of 2-NBDG in Na_x-expressing cells in the 170 mM Na solution was completely inhibited by ouabain, a specific inhibitor of Na^+/K^+-ATPase.

Next, I tested the effect of overexpression of the Na_x-binding fragments of α1 and α2 subunits of Na^+/K^+-ATPase in C6M16 cells, because these fragments are expected to work as a competitor of Na^+/K^+-ATPase for binding to Na_x channels. As was expected, the transfection of an expression vector carrying the fragments of the α1 and α2 subunits significantly suppressed the metabolic response in the C6M16 cells with Na_x expression in the 170 mM Na solution. In contrast, overexpression of the fragment of the α3 subunit, which was negative for interaction with Na_x channel, did not affect the metabolic activation.

The C-terminal fragment of Na_x was also expected to work as a competitor for the binding of Na_x channels to Na^+/K^+-ATPase. Unexpectedly but intriguingly, overexpression of the C-terminal fragment of Na_x further enhanced the 2-NBDG uptake, when it was coexpressed in Na_x-positive cells. This suggests that the C-terminal region of Na_x is also able to support Na^+/K^+-ATPase, as well as the native Na_x. However, the expression of the C-terminal fragment of Na_x by itself (without concomitant expression of the native Na_x) exerted no effect on the 2-NBDG uptake. This strongly suggests that a function of the native Na_x channel (presumably Na^+-influx activity) is also essential for the upregulation of the metabolic state, in addition to the function which is

substitutable with the C-terminal region of Na_x.

To estimate the contribution of Na^+ influx itself to the metabolic activation, I tested the effect of the influx generated by a Na-specific ionophore, monensin, on the uptake of glucose. At a concentration of 0.5 μM, monensin triggered a small Na^+ influx into cells comparable to that of the C6M16 cells expressing Na_x when stimulated in the 170 mM solution. However, the application of 0.5 μM monensin to C6M16 cells without Na_x-channel expression did not enhance the 2-NBDG uptake, and higher concentrations of monensin were not effective either. In contrast, when Na_x-expressing cells were treated with 0.5 μM and higher concentrations of monensin, the 2-NBDG uptake was markedly enhanced dose-dependently. These results clearly indicate that the increase of the Na-ion concentration in the cell is not enough by itself to trigger the uptake of glucose (metabolic stimulation), and that the presence of Na_x channel protein is required for the stimulation of glucose uptake by the cells. Importantly, the C-terminal fragment of Na_x induced markedly enhanced 2-NBDG uptake under the condition without Na_x-channel expression with 0.5 μM monensin. This indicates that the full-length Na_x channel can be replaced by the C-terminal fragment under the condition where Na^+ influx was secured by monensin. Taken together, it is probable that both pre-stimulation of Na^+/K^+-ATPase (by interaction with Na_x channels through the C-terminal region of Na_x) and Na^+ influx (through Na_x channels or monensin) are essential for the activation of the Na^+/K^+-ATPase and the cellular metabolic stimulation.

To examine whether the Na_x channel is indeed involved in the energy-control system in the Na_x-positive glial cells *in vivo*, I performed an imaging analysis of the uptake of glucose in the SFO using 2-NBDG. In the wild-type SFO, incubated with 2-NBDG in the 170 mM Na solution, an intensively labeled mesh-like structure became

apparent, suggesting that fine glial processes in the SFO actively took up the fluorescent derivative of glucose. These results clearly indicate that the SFO tissue has activity to take up glucose in response to a Na-level increase, and the Na_x channel is an essential component for this mechanism.

Next, I examined the dissociated cells from the SFO of wild-type and Na_x-KO mice to confirm that the cells showing the enhancement of 2-NBDG uptake express Na_x channels. Only among the wild-type cells, cellular populations that intensively took up 2-NBDG in the 170 mM Na solution were present, and these cells were all positive for Na_x and GFAP. These results clearly indicate that the Na_x channel is an essential component for the upregulation of energy demand in the SFO under the high Na condition, as observed in the C6M16 cells. In support of this view, cells dissociated from the SFO of wild-type mice showed a markedly enhanced uptake of 2-NBDG in the presence of 0.5 μM monensin, while the same stimulation of the cells from *Na*$_x$-KO mice induced little enhancement of the uptake.

Increased demand for glucose by cells means that cellular glycolysis is enhanced to yield lactate (or pyruvate). To confirm this idea, I next measured the amounts of lactate and pyruvate released from the SFO as another parameter of the metabolic activity. The SFO tissues removed from mice of both genotypes were incubated in a modified Ringer solution (containing 145 mM or 160 mM Na) at 37°C for 30 hr. The wild-type SFO showed an increase in lactate secretion by ~60% compared with the *Na*$_x$-KO SFO, in 160 mM Na solution. On the other hand, amounts of pyruvate released into the medium were 10-fold lower than those of lactate and did not differ under the two different Na conditions. This indicates that anaerobic glycolysis was stimulated in Na_x-positive glial cells of the SFO under the high Na condition.

Neurons in the SFO of *Na*$_x$-KO mice are hyperactivated under dehydrated conditions compared with wild-type mice. In the SFO, GABAergic neurons are one of the major neuronal types surrounded by Na_x-positive glial cells. Then I examined the neuronal activity of GABAergic neurons in the SFO using patch-clamp techniques in the cell-attached mode. I prepared acute slices containing the SFO from *GAD-GFP* mice and *GAD-GFP/Na*$_x$-KO, in which the GABAergic neurons bear enhanced green fluorescent protein (eGFP) as marker, and selected the eGFP-positive cells under a fluorescence microscope. The GABAergic neurons in the SFO of both wild-type and *Na*$_x$-KO mice showed spontaneous firing at a similar frequency (~4 Hz) under the 145 mM Na condition. After the extracellular Na-concentration was raised to 160 mM, the firing frequency of the GABAergic neurons in the SFO of wild-type mice gradually increased 2-fold, but that of *Na*$_x$-KO mice did not show a significant change.

Because metabolic activation leads to the release of lactate from Na_x-positive glial cells, I next checked the possibility that lactate mediates the signal from the glial cells to GABAergic neurons to control the SFO activity. When lactate was added at 1 mM to the perfusate, the firing frequency of GABAergic neurons in the SFO of both wild-type and *Na*$_x$-KO mice increased. Furthermore, when 1 mM of lactate was added under the high Na condition, no additive effect on the neuronal activity was observed. These results indicate that lactate and Na share a common pathway in the stimulation of GABAergic neurons in the SFO. Lactate was most effective at ~1 mM in promoting the firing rate, and at higher concentrations, the firing was rather suppressed.

The neural activation induced by the Na-level increase was inhibited by α-Cyano-4-hydroxycinnamic acid, an inhibitor of monocarboxylate transporters (MCTs). These results clearly indicate that the Na-dependent stimulation of GABAergic neurons

is largely mediated by MCTs. I also examined the effect of the other metabolic monocarboxylates, pyruvate and acetate, both known to be transported by MCTs. When pyruvate was added at 1 mM to the perfusate, the firing frequency of GABAergic neurons in the SFO of both wild-type and *Na_x*-KO mice similarly increased. By contrast, when acetate was added at 1 mM to the perfusate, the firing frequency was not significantly changed in either genotype.

I further explored the activation mechanism underlying the increase in the firing rate of the GABAergic neurons. The finding that lactate and pyruvate are equally effective suggests that the GABAergic neurons are energetically stimulated. Moreover, I found that Na-dependent potentiation of the firing activity of the GABAergic neurons were reduced by diazoxide, an opener of the ATP-sensitive K channel (Kir6.2 / K_{ATP} channel): The K_{ATP} channel closes in response to the increase of intracellular ATP level and depolarizes the cell. So, I examined the membrane potential of the GABAergic neurons during the application of lactate or high Na solution. The membrane potential was depolarized by both lactate and Na, and the depolarization effect was expectedly reduced by diazoxide. These data thus support the view that lactate serves as an energy substrate to up-regulate the firing activity of the GABAergic neurons.

From these results, the following cellular mechanism for the signaling from glial cells to neurons became clear. Na-level-dependent Na^+ influx through Na_x and direct interaction between Na_x and Na^+/K^+-ATPase are the basis for activation of Na^+/K^+-ATPase in the glial cells. Activation of Na^+/K^+-ATPase stimulates anaerobic metabolism of glucose by the glial cells, which produces lactate as the end product. There exist GABAergic neurons spontaneously firing in the SFO. Lactate released from the glial cells functions as the substance signaling to the neurons for activation.

To my knowledge, this study is the first to show that glial cells take the initiative in the regulation of neural activity using lactate as a signaling substance.

Table of contents

Abbreviations

AP	area postrema
APV	D-(–)-2-amino-5-phosphonopentanoic acid
BCIP	5-bromo-4-chloro-3-indolyl-phosphate
CBB	coomassie brilliant blue R-250
CCD	charge coupled device
α-CHCA	α-cyano-4-hydroxycinnamic acid
CNS	central nervous system
CSF	cerebrospinal fluid
CVOs	circumventricular organs
dbcAMP	N^6,2'-*O*-dibutyryl cyclic AMP
DIC	differential interference contrast
DMEM	dulbecco's modified eagle medium
Dox	doxycycline
DRG	dorsal root ganglia
EAAT	excitatory amino acid transporter
EDTA	ethylenediamine-*N,N,N′,N′*-tetraacetic acid
FCS	fetal calf serum
GABA	γ (gamma)-aminobutyric acid
GAT	γ (gamma)-aminobutyric acid transporter
GFAP	glial fibrillary acidic protein
GLAST	L-glutamate / L-aspartate transporter
GLT	L-glutamate transporter
GST	glutathione *S*-transferase
HEPES	4-(2-hydroxyethyl)piperazine-1-ethanesulfonic acid
ICV	intracerebroventricular
IP	immunoprecipitation
KO	knockout mouse
MCT	monocarboxylate transporter
ME	median eminence

MnPO	medial preoptic
Na	sodium
NBT	4-nitroblue tetrazolium chloride
2-NBDG	2-(*N*-(7-nitrobenz-2-oxa-1,3-diazol-4-yl)amino)-2 deoxyglucose
NBQX	2,3-dioxo-6-nitro-1,2,3,4-tetrahydrobenzo[f]quinoxaline-7-Sulfonamide
NHP	neurohypophysis
NNC711	1,2,5,6-tetrahydro-1-[2-[[(dyphenylmethylene)amino]oxy] ethyl]-3-pyridineca rboxylic acid hydrochloride
OVLT	organum vasculosum of the lamina terminalis
PBS	phosphate-buffered salines
PFA	paraformaldehyde
PVN	paraventricular nucleus
SBFI/AM	sodium-binding benzofuran isophthalate acetoxymethyl ester
SDS-PAGE	SDS-polyacrylamide gel electrophoresis
SE	standard error
SFO	subfornical organ
SNAP5114	1-[2-[*tris*(4-methoxyphenyl)methoxy]ethyl]-(*S*) -3-piperidinecarboxylic acid
SON	supraoptic nucleus
S1	first transmembrane segment
S4	fourth transmembrane segment
S6	sixth transmembrane segment
TBOA	DL-*threo*-β-benzyloxaspartic acid
TPI	triose-phosphate isomerase
TRE	tetracycline-responsive element
TTX	tetrodotoxin
VHC	ventral hippocampal commissure
3V	third ventricle
WT	wild-type mouse
[Na^+**]**	sodium concentration

$[Na^+]_i$	intracellular sodium concentration
$[Na^+]_o$	extracellular sodium concentration

List of Figures

Chapter I

Chapter II

Chapter III

Chapter IV

Chapter V

Chapter I

General introduction

Na sensor is postulated to exist in the sensory circumventricular organs

Sodium (Na) is a major electrolyte of the extracellular fluids and the main determinant of osmolarity. Because Na homeostasis is essential to life, Na-ion concentrations in plasma and CSF are continuously monitored to maintain a physiological level of Na in body fluids. A specific Na sensor has been long hypothesized to exist in the brain for the control of Na intake (Denton *et al*., 1996; Weisinger *et al*., 1979) as well as natriuresis (Cox *et al*., 1987; Denton *et al*., 1996). The site for the sensing was postulated in the circumventricular organs (CVOs) in the periventricular region of the brain (Cox *et al*., 1987; Denton *et al*., 1996; Park *et al*., 1989). The CVOs, midline structures found in the brain of all vertebrates (McKinley *et al*., 2003), are so named because of their proximity to the ventricles of the brain. They are situated in the walls of the ventricle and are accessed by the CSF via a single layer of specialized ependymal cells. In addition, they have characteristic structures of permeable capillary networks that lack blood-brain barrier and facilitate tissue penetration of circulating substances (Johnson and Gross, 1993). Among the CVOs, only three loci, the subfornical organ (SFO), organum vasculosum of the lamina terminalis (OVLT), and area postrema (AP) harbor neuronal cell bodies, which have efferent neural connections to many other areas of the brain. Their neurons are supposedly exposed to the chemical environment of the general circulation, unlike other neuronal perikarya in the CNS, because of the lack of a normal blood-brain barrier. Therefore, these three CVOs are termed sensory circumventricular organs (Fig. I.1; Johnson and Gross, 1993). As for Na, the anterior wall of the third ventricle, where the SFO and OVLT take place, has been suggested to be involved in Na sensing (Andersson, 1978; Denton *et al*., 1996; Johnson *et al*., 2003).

***Na$_x$*-KO mice shows abnormal Na-intake behaviors**

Na_x is an atypical Na channel with low homology (~50% identical) to other voltage-gated sodium channels (Fig. I.2; Goldin *et al*., 2000). It shows significant amino acid sequence differences in the voltage sensors compared with voltage-gated sodium channels: Na_x lacks some positive charges in the S4 segment, which are important for voltage sensitivity. The amino acid sequences in the inactivation gate and pore regions which are critical for channel function in voltage-gated sodium channels are

not conserved either (George *et al*., 1992). In addition, all the attempts to express functional Na_x channels using heterologous expression systems such as Xenopus oocytes, Chinese hamster ovary cells, and human embryonic kidney 293 cells, have been unsuccessful (Felipe *et al*., 1994; Akopian *et al*., 1997). To examine the functional role of Na_x *in vivo*, Prof. Noda's laboratory generated a mouse line in which the *Na_x* gene was knocked-out by insertion of the *LacZ* gene in-frame (Watanabe *et al*., 2000). In these mice, the *lacZ* gene is expressed in place of the *Na_x* gene and one can detect the loci of *Na_x* expression by X-gal staining. The *lacZ* expression was limited to specific loci including four CVOs, the SFO, OVLT, median emincence (ME), and posterior pituitary (Fig. I.3; Watanabe *et al*., 2000).

If the Na_x channel has some functional roles in the sensory circuits for body-fluid homeostasis, the neural activity and gene expression in these organs would be affected in the *Na_x*-gene knockout (*Na_x*-KO) mice. They examined the effects of water deprivation on the expression of a nuclear protein, Fos, the product of the *c-fos* proto-oncogene (Fig. 1.4; Watanabe *et al*., 2000). Fos is a marker of changes in neural activity in response to the extracellular fluid balance in mice and rats (Ueta *et al*., 1995; Chae and Heideman, 1998; Morien *et al*., 1999). Fig. I.4B shows the time course of changes in Fos-immunopositive cell density under water-satiated and dehydrated conditions. In the water-satiated condition, Fos-immunopositive cells were not detected in WT and *Na_x*-KO mice. As the duration of water deprivation increases, cell numbers with Fos-immunopositive nuclei were remarkably increased in the SFO and OVLT but not in other regions (SON, MnPO, PVN, data not shown).

They next examined the preference to hypertonic saline (0.3 M NaCl). In the dehydrated condition, animals take in a large quantity of water and avoid hypertonic saline to recover from the hypertonic state. However, *Na_x*-KO mice did not stop ingesting salt when dehydrated, while WT mice avoided salt (Fig. I.5; Hiyama *et al*., 2004; Watanabe *et al*., 2000). They further examined the effects of the direct stimulation of CVOs with hypertonic Na solutions from the cerebral ventricle on drinking behavior in the two-bottle test. They showed that salt aversive behavior does not occur on direct infusion of a hypertonic Na solution (0.5 M NaCl) into the cerebral ventricle in *Na_x*-KO mice in contrast to wild-type mice (Fig. I.6; Hiyama *et al*., 2004).

The behavioral phenotype of *Na$_x$*-KO mice was completely recovered by a site-directed transfer of the *Na$_x$* gene with an adenoviral vector into the SFO (Fig. I.7; Hiyama *et al*., 2004). All these findings indicate that the Na_x channel is the brain Na-level sensor (Noda, 2006), that was postulated to be present in the CVOs involved in the regulation of water/salt-intake (Andersson, 1978). These results led them to propose Na_x is involved in the sodium-level sensing mechanism in the brain.

Na_x is equipped with molecular properties for the Na-level sensor

Next, the molecular properties of Na_x expressed in the SFO were explored by imaging analysis. When the extracellular sodium-ion concentration ($[Na^+]_o$) was raised stepwise from the normal amount, they examined the intracellular sodium-ion concentration ($[Na^+]_i$). When $[Na^+]_o$ was increased from the control amount of 145 mM (physiological level) to 170 mM by bath application, the $[Na^+]_i$ of some cells dissociated from the SFO of wild-type mice showed a pronounced increase (Fig. I.8A). Importantly, all the responsive cells were Na_x-immunoreactive. In contrast, some Na_x-immunonegative cells dissociated from the SFO did not show such response. These data indicates that the Na_x channel is a concentration-sensitive Na channel with a threshold value of approximately 150 mM for the extracellular Na ion (Fig. I.8B; Hiyama *et al*., 2002). The sensitivity and threshold of Na_x channels to the extracellular Na-level is in a range of physiological change: sodium concentrations and plasma osmolarity increase by 5–10% during thirst conditions (Wakerley *et al*., 1978; Nose *et al*., 1992).

Na_x is expressed in glial laminate processes in the sensory CVOs

More recently, they tried to identify the cellular population expressing Na_x channels in the sensory CVOs by double-immunostaining and immunoelectron microscopic analyses. They found that Na_x channels are specifically expressed in perineuronal processes of astrocytes and ependymal cells enveloping particular neural populations in the sensory CVOs (Fig. I.9; Watanabe *et al*., 2006). In addition, glial cells isolated from the subfornical organ, one of the CVOs, were sensitive to an increase in the extracellular

sodium level, as analyzed by an ion-imaging method. These findings indicate that the Na_x-expressing glial cells are the primary site of sodium-level sensing, and suggest a signaling mechanism by which the Na-increase sensed by "inexcitable" glial cells is transferred to neurons. A specific neuron-glia communication regulated by Na_x channel is implicated in the ingestion control for the salt/water homeostasis.

In this study, I tried to reveal this mechanism using multidisciplinary approaches, and eventually found that lactate-based signaling from Na_x-positive glial cells to neurons is involved in the sensing mechanism of the Na level in body fluids.

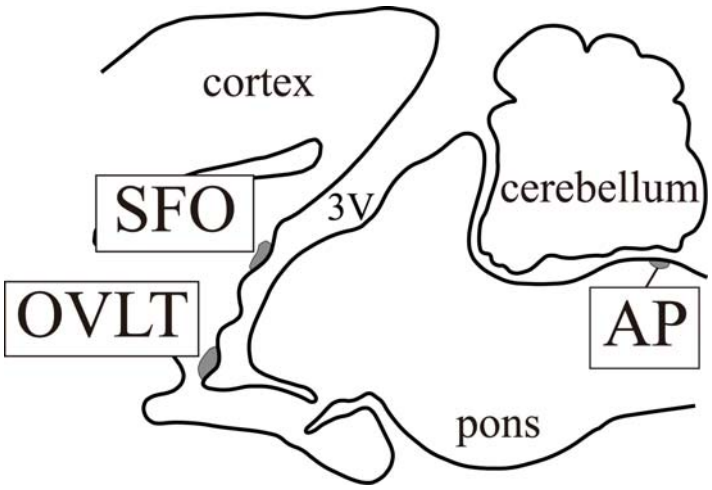

Fig. I.1. Sensory circumventricular organs.

The sensory circumventricular organs (CVOs) in the midsagittal section of the mouse brain are schematically represented. Those three loci are midline structures situated in the wall of third and fourth ventricles. Among CVOs, only sensory CVOs harbor neuronal cell bodies. SFO, subfornical organ; OVLT, organum vasculosum laminae terminalis; AP, area postrema; 3V, third ventricles.

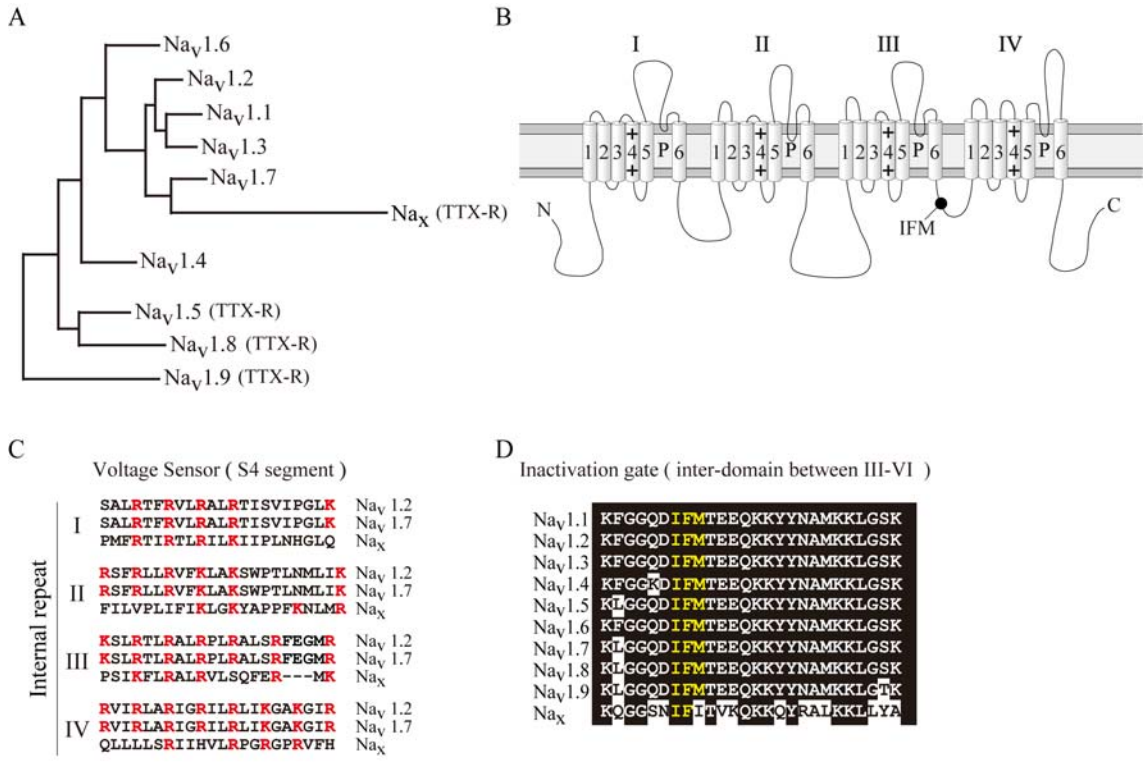

Fig. I.2. Na$_x$ channel is a member of the sodium channel family.

(A) Phylogenetic relationships of rat sodium channel sequences Na$_v$1.1–1.9 and Na$_x$. TTX-R : tetrodotoxin resistant sodium channels.

(B) Putative transmembrane topology of sodium channel α subunits. 1–6, putative transmembrane segment (S1–S6) in each repeat (I–IV); P, pore region; IFM, a critical motif for the fast inactivation.

(C) Alignments of S4 segments of rat Na$_v$1.2, Na$_v$1.7, and Na$_x$. Na$_x$ lacks some positively-charged amino acids (red) in the S4 segment, which are important for voltage sensitivity.

(D) Inter-domains between III–VI of rat Na$_v$1.1–1.9 and Na$_x$. The amino acid sequences in Na$_x$ for the inactivation gate which are critical for the fast inactivation in voltage-gated channel are not conserved. Yellow : IFM, a critical motif for the fast inactivation.

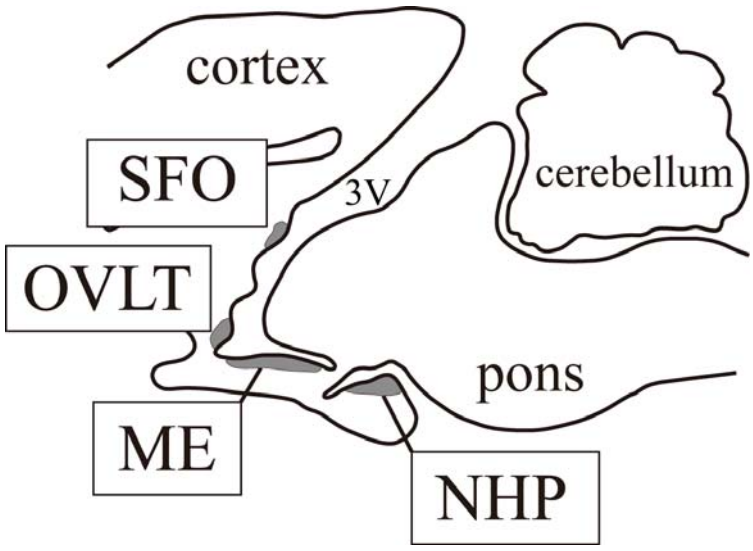

Fig. I.3. Na_x was expressed in specialized region of the adult CNS.

LacZ expression was analyzed in *Na_x*-KO mice, in which *Na_x* is replaced by *lacZ*. The *Na_x*-positive circumventricular organs (CVOs) in the midsagittal section are schematically represented. SFO, subfornical organ; OVLT, organum vasculosum laminae terminalis; ME, median eminence; NHP, neurohypophysis; 3V, third ventricle.

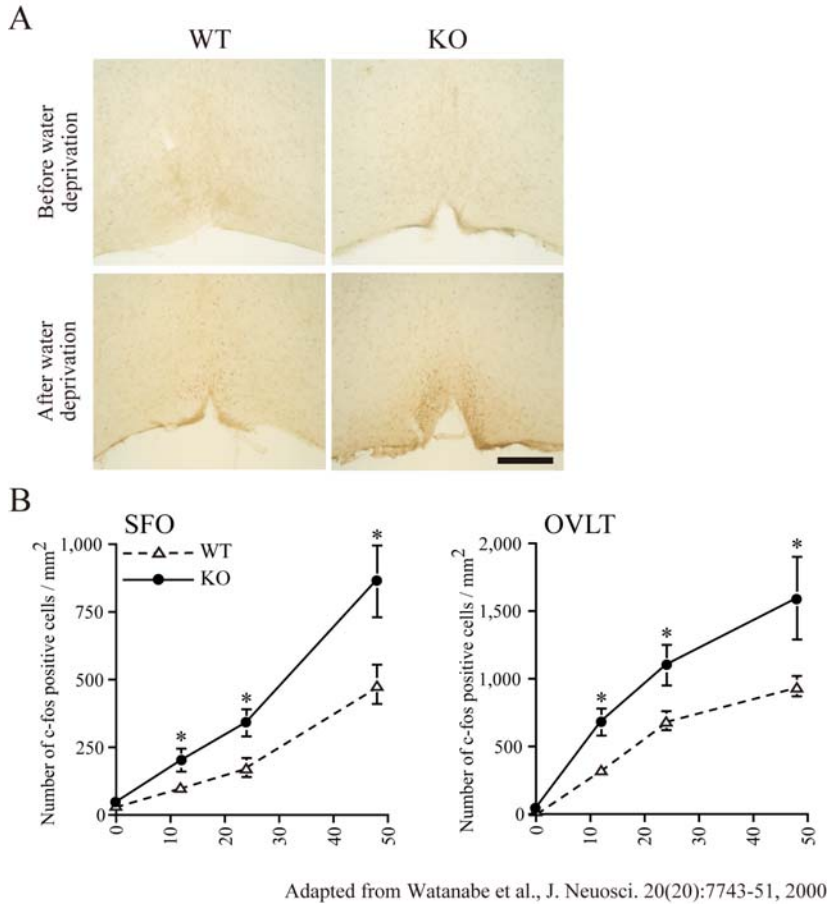

Fig. I.4. Abnormal increase of Fos-immunopositive nuclei were selectively observed in the SFO and OVLT of the *Na*$_x$-KO mice under dehydrated conditions.

(A) Typical examples of tissue sections containing the OVLT derived from euhydrated or 24-hour dehydrated wild-type (WT) and *Na*$_x$-KO (KO) mice. Scale bar, 200 μm. WT or *Na*$_x$-KO mice were dehydrated for 0, 12, 24 and 48 hours and then fixed. The fixed brains were cut coronally into 50 μm thick sections and stained with anti-Fos polyclonal antibody.

(B) Mean numbers of Fos-immunopositive cells per square millimeters in the SFO, OVLT, during water deprivation were plotted. Data are mean and SE. * $P < 0.05$, two-tailed t test (against WT). SFO, subfornical organ ; OVLT, organum vasculosum laminae terminalis.

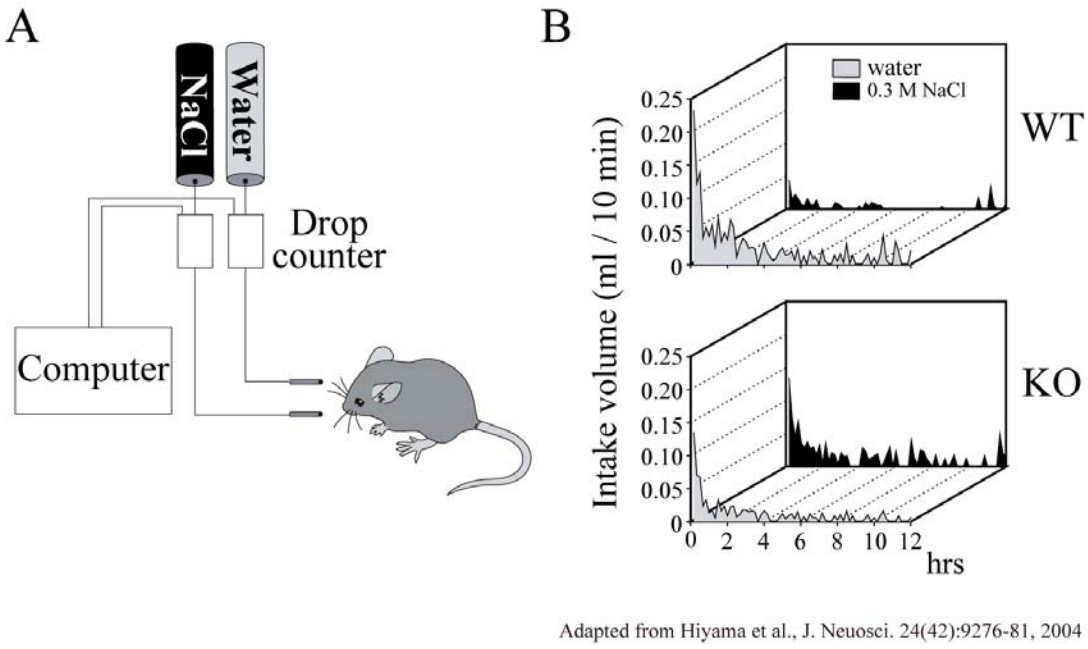

Fig. I.5. ***Na*$_x$-KO mice exhibit abnormal salt-intake behavior under dehydrated conditions.**

(A) Schematic representation of the experimental setup for the two-bottle test.

(B) Averaged time course of water and saline (0.3 M NaCl) intake in wild-type (WT) and *Na*$_x$-KO (KO) mice during the dark phase immediately after 48 hours of dehydration. After dehydration, animals of both genotypes rushed to drink fluids in large amounts, and subsequently, the drinking rate decreased gradually. When dehydrated, WT mice preferred pure water and avoided the hypertonic saline. In contrast, *Na*$_x$-KO mice took both pure water and 0.3 M NaCl equally. Each point shows the average quantity per 10-minute period. n = 10.

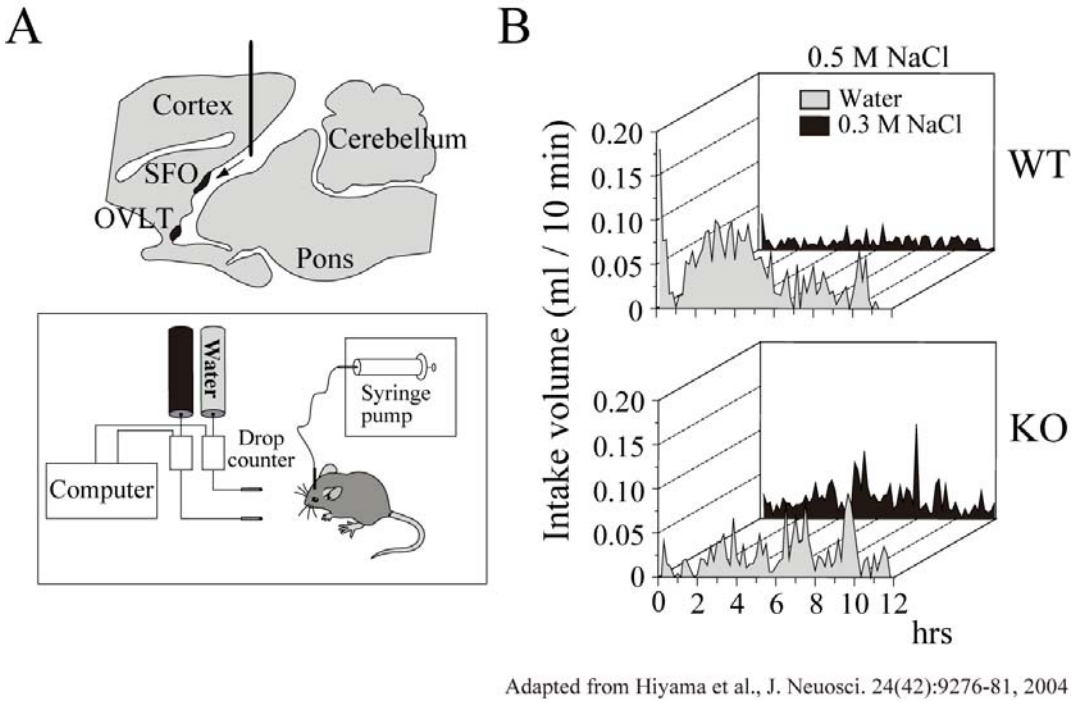

Fig. I.6. *Na$_x$*-KO mice are insensitive to increases of the Na level in the CSF.

(A) Direct stimulation of CVOs with hypertonic Na solutions from the cerebral ventricle during the two-bottle test. Location of the cannula for intracerebroventricular microinfusions (top). The tip of the cannula was positioned at the lateral ventricle. A schematic representation of the experimental setup for the two-bottle test (bottom). Two drinking tubes were presented to free-moving mice infused with sodium solutions into the cerebral ventricle for 12 hours.

(B) Averaged time course of water and saline (0.3 M NaCl) intake in wild-type (WT) and *Na$_x$*-KO (KO) mice during intracerebroventricular (ICV) infusions of a hypertonic (0.5 M) NaCl solution. When the hypertonic saline (0.5 M NaCl) was continuously infused into the cerebral ventricle, WT mice clearly avoided the salt solution. In contrast to the WT, the *Na$_x$*-KO mice did not show such an aversion to the salt solution. Each point shows the average quantity per 10-minute period. n =10. SFO, subfornical organ; OVLT, organum vasculosum laminae terminalis.

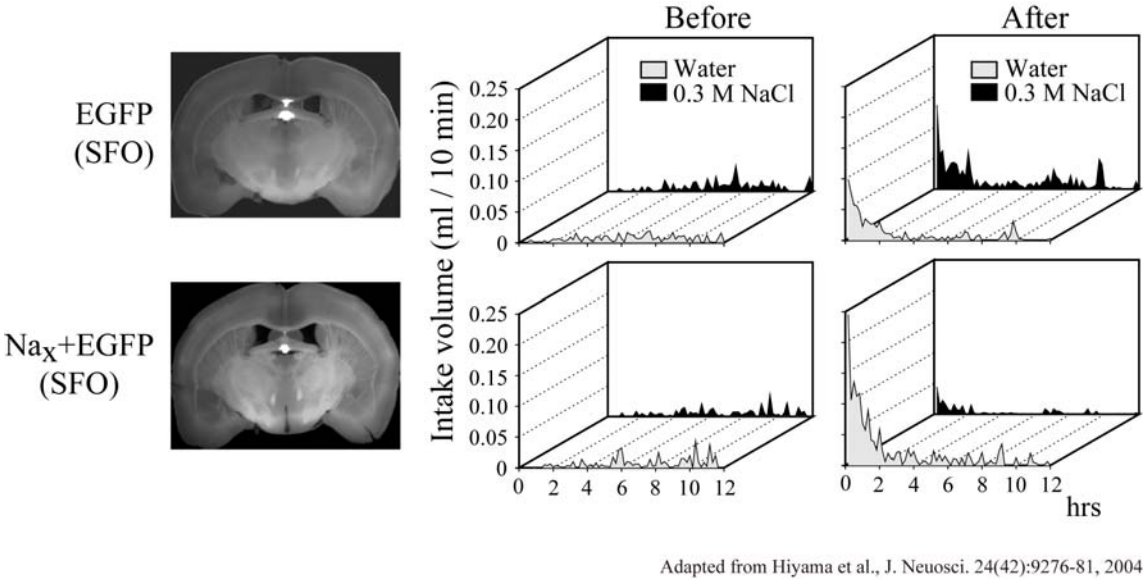

Fig. I.7. Abnormal salt-intake behavior of *Na_x*-KO mice was rescued by introduction of the *Na_x* gene to SFO.

Na_x gene was locally introduced into the brain of the *Na_x*-KO (KO) mice with an adenoviral expression vector carrying *Na_x* under the control of the cytomegalovirus promoter. An adenoviral expression vector encoding the *egfp* gene was coinjected to identify the infected site after the experiments. One week after the injection, the mice were subjected to the behavioral tests to examine whether Na-aversion behavior was rescued.

Among the *Na_x*-KO mice that received the *Na_x* gene together with the *egfp*, six showed the Na aversion as in the wild-type (WT) mice when dehydrated. The infected regions in these mice were then analyzed. All of the 6 mice that were conferred with the Na-aversion behavior showed a common infection finely in the SFO (Na_x + EGFP). The coronal sections of the brain showing the loci infected by the expression of EGFP (*left* column). Time course of water and saline (0.3 M NaCl) intake by the infected mice before and after 48 hours of dehydration (*middle* and *right* columns, respectively). Behavioral data are the average of six mice that were successfully infected at a specific site in the brain by an adenoviral vector encoding *egfp* (EGFP) or by vectors encoding *egfp* and *Na_x* (Na_x + EGFP). SFO, subfornical organ.

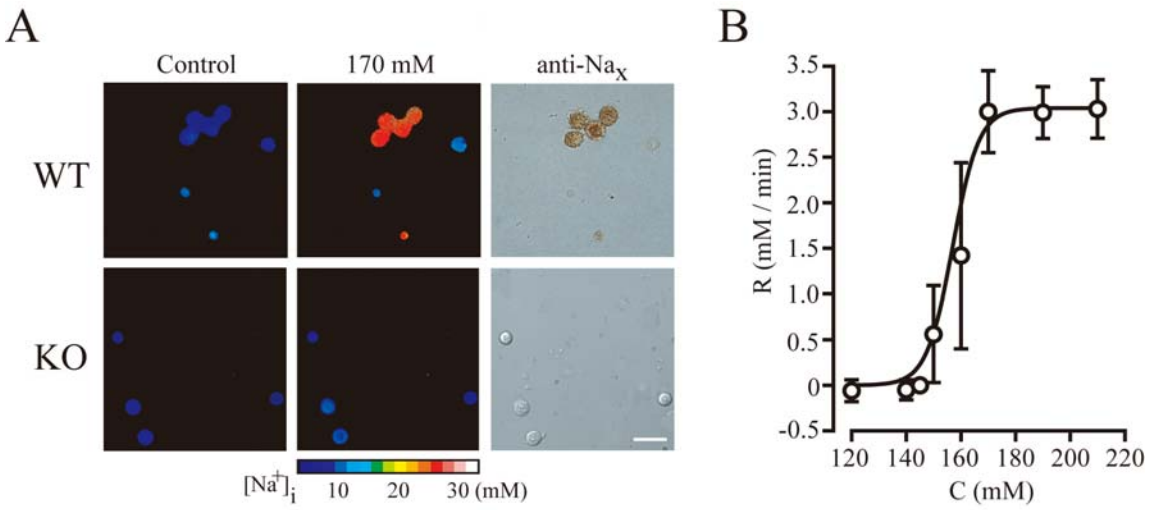

Adapted from Hiyama et al., Nature Neuroscience, 5(6) 511-512, 2002

Fig. I.8. Na_x channel is a concentration-sensitive Na channel.

(A) Pseudocolor images showing the intracellular Na concentration ($[Na^+]_i$) of the cells in the control and 170 mM Na solutions. When extracellular Na concentration ($[Na^+]_o$) was increased from the control amount of 145 mM to 170 mM by bath application of NaCl solution, the $[Na^+]_i$ of dissociated SFO cells derived from wild-type (WT) mice showed a pronounced increase from ~10 mM to ~30 mM. All the responsive cells in this region were also Na_x-immunoreactive cells. In contrast, no SFO cells derived from *Na_x*-KO (KO) mice showed such responses. Scale bar, 50 μm.

(B) Relationship between the $[Na^+]_i$ increase rate (R) and $[Na^+]_o$. R was calculated from the slope between 20% and 80% of maximum $[Na^+]_i$. The solid line is the fit of the data to the equation $R = R_{Max}/(1 + \exp((C_{1/2} - C)/a))$, where $C = [Na^+]_o$. The values R_{Max} = 3.04 mM/min, $C_{1/2}$ = 157 mM and a = 4.67 mM were used; n = 21.

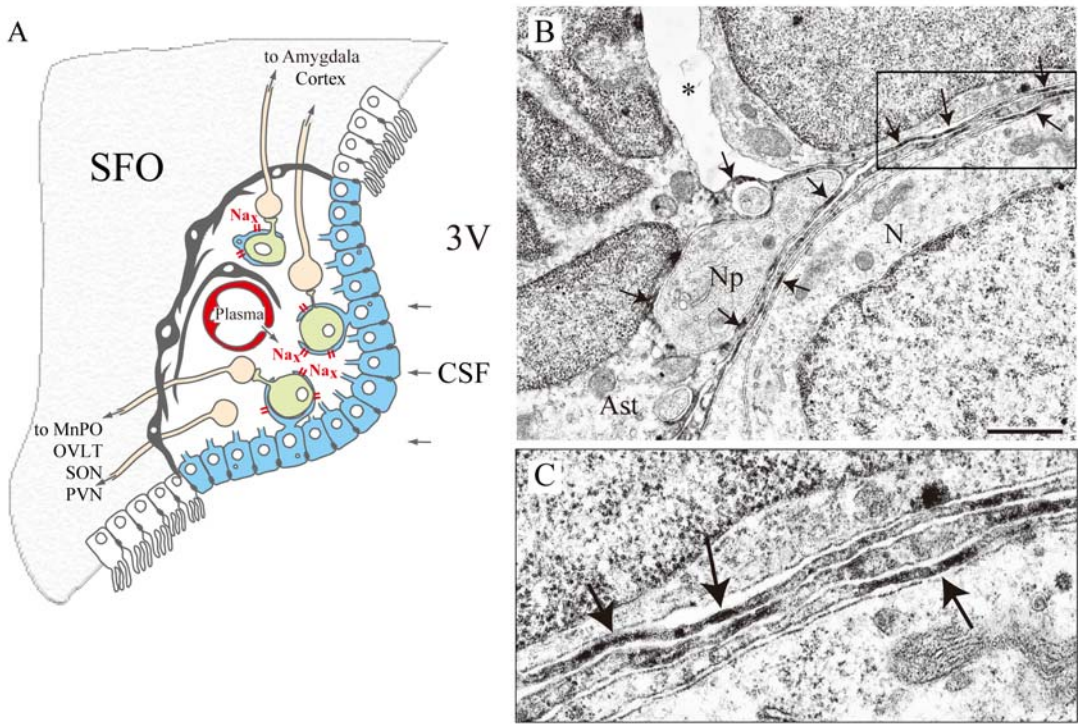

Adapted from Watanabe et al., Am. J. Physiol. Regul. Integr. Comp. Physiol 290:R568-76, 2006

Fig. I.9. The Na_x channel is expressed in perineuronal processes of astrocytes and ependymal cells in the SFO.

(A) Schematic representation of the SFO and Na_x channels. The features of SFO are extensive vascularization, no blood-brain barrier, and atypical ependymal cells. SFO, subfornical organ; OVLT, organum vasculosum laminae terminalis; 3V, third ventricles; CSF, cerebrospinal fluid; MnPO, median preoptic; SON, supraoptic nucleus; PVN, paraventricular nucleus.

(B and C) Immunoelectron microscopic image of the core regions of the SFO. Neurons and their processes are surrounded by immunopositive thin processes of astrocytes (B). These immunopositive thin lamellate processes extended from cell bodies of astrocytes in B is magnified in C. The asterisk in B indicates an artificial void region produced during fixation or staining. Ast, astrocyte; Np, neuronal process; N, neuron. Scale bar: 1 μm.

Chapter II

Na_x channels directly interact with the α-subunits of Na^+/K^+-ATPase

II.1 Introduction

As referred in Chapter I, I hypothesized that there exist some signaling mechanisms by which the Na signal sensed by glial cells is transferred to neurons in the SFO. To find a clue to the mechanism for the glia-neuron transmission in the Na-sensing, I tried to reveal the physiological role of Na_x in the glial cells. I screened for molecules interacting with Na_x using the yeast two-hybrid system with each of the cytoplasmic domains of mouse Na_x as bait. I found several candidate molecules that interact with Na_x, including cytoskeletal protein, ionic pump, phosphatase, Ca^{2+} binding protein, motor protein, proteasome subunit, intracellular signaling protein, and house-keeping cytosolic enzyme. Among them, I selected α subunit Na^+/K^+-ATPase for subsequent analysis, because Na_x and Na^+/K^+-ATPase are supposed to be relevant through Na influx to the cell. Na influx is proposed as an activating stimulus of Na^+/K^+-ATPase (Pellerin *et al*., 1998). It implies the possibility of colocalization in the membrane and direct functional coupling between the two. I then examined the interaction between Na_x and Na^+/K^+-ATPase by several biochemical approaches.

II.2 Materials and Methods

cDNA library and yeast two-hybrid screening

Adult wild-type mice were deeply anesthetized with diethyl ether before decapitation. The dorsal root ganglia (DRG) were removed, and total RNA was extracted using Trizol reagent (Invitrogen, Carlsbad, CA). Messenger RNA was isolated using Dynabeads (Invitrogen). A DRG cDNA library was generated by using the SuperScript Choice System for cDNA Synthesis (Invitrogen) according to the instruction manual using the pACT2 prey vector to express fusion proteins with the GAL4 transcription-activating domain (approximately 8 x 10^5 independent clones).

DNA fragments encoding the cytoplasmic regions of mouse Na_x channels (amino acids: 1–116, 394–504, 724–932, 1186–1251, and 1489–1681) were individually inserted into the pBTM116 bait plasmid (Bartel and Fields, 1995; Vojtek and Hollenberg, 1995) to express as an in-frame fusion protein with the LexA DNA-binding domain. *Saccharomyces cerevisiae* strain L40 cells (Vojtek *et al*., 1993) were transformed with the bait plasmids, and transformants were selected based on growth on plates of a synthetic dropout medium lacking tryptophan (nacalai tesque, Kyoto, Japan). Yeast two-hybrid screening was performed according to the manufacturer's directions (Yeast Protocols Handbook; Clontech). Briefly, the L40 cells transformed with both the bait plasmid and prey plasmid were selected based on growth on plates of synthetic dropout medium lacking tryptophan, leucine, and histidine but containing 3 mM 3-aminotriazole by incubation for six days at 30 °C. Approximately 3 x 10^6 clones were screened using a mouse DRG cDNA library. Positive clones were selected by conducting a β-galactosidase filter-lift assay at 30°C for two days according to the manufacturer's directions (Yeast Protocols Handbook; Clontech).

Plasmid DNAs were recovered from the positive clones, and retransformed individually into L40 cells to verify the positive phenotype. The nucleotide sequences of positive clones were determined by a DNA sequence analyzer (3100, Applied Biosystems, Foster City, CA), and the identity of the putative interacting proteins encoded in the positive clones was determined by data base searches

(Nucleotide-nucleotide BLAST, NCBI). Using the C-terminal region of Na_x as bait, I identified three Na^+/K^+-ATPase α1 clones encoding an identical region (amino acid residues 596–717: GenBank accession number BC042435).

For analyzing the interaction between the C-terminal region of Na_x and α subunits of Na^+/K^+-ATPase, DNA fragments encoding the mouse α2 (593–714 of BC036127) and α3 (586–707 of BC037206) subunits were individually inserted into the pACT2 prey plasmid to express fusion proteins with the GAL4 transcription-activating domain. A filter-lift β-galactosidase assay was performed as described above.

Immunoprecipitation

Preparation of cellular membrane proteins was performed as described (Garty *et al*., 2002; Jewell and Lingrel, 1991) with some modifications. Briefly, C6M16 cells (1.8×10^7) were homogenized in 1.2 ml of 1 mM $NaHCO_3$, 2 mM $CaCl_2$, and 5 mM $MgCl_2$, and centrifuged at 3,000 *g* for 5 min. The supernatant was treated with 1 M NaI for 10 min, and membranes were precipitated by centrifugation at 48,000 *g* for 30 min. The membranes were washed twice with a buffer containing 25 mM imidazole, 20 mM Tris-HCl, 50 mM NaCl, and 1 mM EDTA (pH 7.4), and suspended in 500 μl of the same buffer. Membrane proteins were solubilized by adding $C_{12}E_{10}$ (decaethylene glycol monododecyl ether, Sigma) to a final concentration of 1 mg/ml. After centrifugation at 100,000 *g* for 30 min, the supernatant was used for immunoprecipitation. The supernatant (250 μl) was incubated with anti-Na^+/K^+-ATPase α1 mouse monoclonal antibody (clone 6H, 1:250 dilution, Upstate Biotechnology, Lake Placid, NY) or control antibody (mouse monoclonal anti-HA antibody, clone HA-7, Sigma) for 3 hr. Protein G Sepharose (20-μl volumes, pre-washed with a buffer containing 1 mg/ml of $C_{12}E_{12}$ and 1% polyvinylpyrrolidone) was added, and the suspensions were further incubated with swirling for 1 hr. The immunoprecipitates were washed four times with the buffer containing 1 mg/ml of $C_{12}E_{10}$, and subjected to immunoblotting analysis as described (Fujikawa *et al*., 2003). All experiments were performed below 4°C.

Pull-down experiment

I performed pull-down experiments using glutathione *S*-transferase (GST) fusion proteins of the carboxyl-terminal region (amino acid residues 1,489–1,681) of Na_x (GST-Na_x-C-term). I used the pGEX expression vector system and GST trap FF column (GE healthcare, Piscataway, NJ) to prepare GST-Na_x-C-term proteins. To generate expression plasmid for His-tagged fragment of the α1 subunit of Na^+/K^+-ATPase (His_6-Na^+/K^+α1), the corresponding cDNA region (amino acid residues 591–759) was amplified by PCR using mouse cDNA of the α1 subunit of Na^+/K^+-ATPase as template with primers containing a EcoRI site (5'-tgaattcatgattgaccctccccgagctgc-3') and SalI site (5'-agtcgacgctttcttcaagttatcaaaaatcag-3'). The cDNA fragment excised by *Eco*RI and *Sal*I digestion was inserted into the EcoRI and SalI sites of pET-28a (Novagen, San Diego, CA). His_6-Na^+/K^+α1 was expressed in *E. coli* BL-21(DE3) and purified by metal chelate chromatography (His-Bind purification kit, Novagen). For the pull-down assay, 20 μl of glutathione sepharose beads coated with 2 μg of GST-Na_x-C-term or GST were incubated with tissue lysate (200 μg protein) prepared by extraction with 1% Triton X-100 from the mouse brain membrane fraction (Maeda *et al*., 1994) or with purified His_6-Na^+/K^+α1 (2 μg), in 400 μl of 50 mM Tris-HCl, pH 7.5, 150 mM NaCl, and 1% Triton X-100 overnight at 4°C. After washing the beads, the bound proteins were eluted by boiling in the SDS-PAGE sample buffer and subjected to immunoblotting analysis.

Immunohistochemistry of brain sections

The cryostat sections were incubated with 25 mM glycine in PBS for 30 min and pretreated with 5% serum in PBS containing 0.1% Triton X-100 (PBST) overnight at 4°C. They were then incubated with a mixture of primary antibodies (anti-Na_x rabbit antiserum at a 1:1000 dilution, and Na^+/K^+-ATPase α1 mouse monoclonal antibody at 5 μg/ml) in the blocking buffer for 2 days at 4°C. The sections were washed 3 times with PBST and then incubated with fluorescent dye-conjugated secondary antibodies (Alexa488-conjugated anti-mouse antibody, 1:500; and Alexa594-conjugated anti-rabbit

antibody, 1:500; Molecular Probes, Eugene, OR) overnight at 4°C. They were then washed 3 times with PBST, mounted, and observed under a fluorescence microscope.

Dissociation culture of the SFO cells

Adult wild-type mice (8–16 wk old: n = 10) were deeply anesthetized with diethyl ether and decapitated. The SFOs were then excised from the brains. Dissociation of the SFO was performed as previously reported (Hiyama *et al*., 2002). Isolated cells were plated on glass-bottom dishes (Matsunami Glass, Kishiwada, Japan) coated with Cell-tak (BD Biosciences, NJ), and incubated in DMEM containing 10% FCS in a humidity-controlled incubator gassed with 5% CO_2 for 3 hr at 37°C.

Immunostaining of dissociated SFO cells

SFO cells on the Cell-tak-coated glass-bottom dishes were washed twice with PBS and fixed in ice-cold methanol for 1 hr. Fixed cells were permeabilized with 0.04 % NP-40 in PBS for 20 min, and then blocked with 4% skim milk in PBS (blocking buffer). The cells were incubated overnight at 4°C with a mixture of primary antibodies in the blocking buffer and washed four times with PBS: for the experiments in Fig. IV.2 in Chapter IV, anti-GFAP antibody (sc-9065; Santa Cruz Biotechnology, Santa Cruz, CA) was used. To detect the binding of specific antibodies, cells were incubated for 1 hr with fluorescent dye-conjugated antibodies, and washed four times with PBS. The antibodies were diluted as described in the immunohistochemistry of brain sections. Cells were mounted with Permafluor (Beckman Coulter Co., Marseille, France) and observed using a Zeiss LSM510 confocal microscope (Carl Zeiss, Jena, German).

***In situ* hybridization**

Templates used for the preparation of probes were the 792-bp fragment of mouse Na^+/K^+-ATPase α1 cDNA (residues 2191–2983, GenBank accession number BC042435), the 469-bp fragment of mouse Na^+/K^+-ATPase α2 cDNA (881–1350, BC036127), and the 303-bp fragment of mouse Na^+/K^+-ATPase α3 cDNA (3201–3504, BC037206).

Mice were anesthetized and perfused with 4% paraformaldehyde (PFA) in PBS. Brains were dissected, fixed overnight at 4°C, and infiltrated with a graded sucrose series. The brains were then embedded in OCT compound (Sakura, Tokyo, Japan) and sectioned at 14 μm with a cryostat (CM3050S, Leica Microsystems, Wetzlar, Germany). Samples were postfixed in 4% PFA for 15 min, washed in PBS for 5 min, and then treated with 10 μg/ml proteinase K for 10 min at room temperature, refixed in the 4% PFA, and acetylated in 0.1 M triethanolamine. After a wash with PBS, the samples were prehybridized for 1 hr, and hybridized for 16 h at 55°C. Digoxigenin-labeled RNA probes were denatured for 5 min at 85°C before use. The hybridization solution was as follows: 0.1 mM EDTA, 10 mM Tris-HCl, pH 7.4, 0.6 M NaCl, 0.1% SDS, 400 μg/ml yeast tRNA, 1× Denhardt's solution, and 10% dextran sulfate. After hybridization, the samples were washed in 4× SSC at 50°C, then digested with 10 μg/ml RNase A for 1 hr at 37°C, and washed in 2× SSC and 0.1× SSC at 50°C. The samples were finally incubated with alkaline phosphatase-conjugated anti-digoxigenin antibodies at room temperature in a humidified chamber and developed with 4-nitroblue tetrazolium chloride (NBT) and 5-bromo-4-chloro-3-indolyl-phosphate (BCIP) overnight. Images were acquired with a CCD camera (DP70, Olympus, Tokyo, Japan) and microscope system.

II.3 Results

Na_x channels directly interact with Na^+/K^+-ATPase

To better understand the physiological processes involving Na_x in glial cells, I screened for molecules interacting with Na_x using the yeast two-hybrid system with each of the cytoplasmic domains of mouse Na_x as bait. Among the positive clones isolated from a mouse DRG cDNA library by using the C-terminal region of Na_x (amino acid residues 1,489–1,681) as bait (Fig. II.1A left), three clones coded for the α subunit of Na^+/K^+-ATPase. A detailed analysis revealed that all these clones were identical and coded for the amino acid residues 596–717 of the α1 isoform, a position close to the cytoplasmic catalytic domain of the α subunit of Na^+/K^+-ATPase (Fig. II.1A, right; Fig. II.1B).

The direct interaction between the C-terminal region of Na_x and the α1 subunit of Na^+/K^+-ATPase was verified by pull-down assays. The interaction between the C-terminal region of Na_x and the catalytic domain of the α1 subunit of Na^+/K^+-ATPase was confirmed by using glutathione S-transferase (GST) pull-down assay. The His-tagged catalytic domain of the α1 subunit of Na^+/K^+-ATPase (amino acid residues 591–759) (His_6-Na^+/K^+α1) and the GST-fusion protein of the C-terminal region (amino acid residues 1,489–1,681) of Na_x (GST-Na_x-C-term) were expressed in *E. Coli* and purified (Fig. II.2). The pull-down assay with the purified His_6-Na^+/K^+α1 showed an direct interaction between the C-terminal region of Na_x and the catalytic domain of the α1 subunit of Na^+/K^+-ATPase (Fig. II.3). The beads coated with GST-Na_x-C-term or GST successfully pulled down the endogenous α1 subunit of Na^+/K^+-ATPase from the brain membrane fraction prepared from wild-type mice (Fig. II.4).

I further examined the interaction between the full-length mouse α1 subunit of Na^+/K^+-ATPase and full-length Na_x protein by establishing C6 cell lines expressing Na_x (C6M16; see next chapter). Following the immunoprecipitation of the cell lysate with a specific antibody (6H antibody) to the α1 subunit of Na^+/K^+-ATPase, a Western blot analysis with anti-Na_x channel antibodies was performed. The 6H antibody efficiently pulled down both Na_x (~200 kDa) and the α1 subunit of Na^+/K^+-ATPase at (~110 kDa)

(Fig. II.5, 6H), demonstrating an interaction between the two proteins in living cells. Anti-HA used as a control antibody did not pull down either the Na_x channel or the α1 subunit of Na^+/K^+-ATPase (Fig. II.5, Con).

Coexpression of the α1 subunit of Na^+/K^+-ATPase and Na_x channels was examined by double-fluorescent immunostaining using sections of the SFO and dissociated cells from the SFO. The α1 subunit was broadly distributed throughout the SFO, overlapping with the expression of Na_x channels (Fig. II.6B). The confocal microscopic analyses with isolated cells from the SFO showed that both molecules were colocalized in the plasma membrane (Fig. II.6H). Na_x channels were expressed in large round cells, but not in small cells with neurite-like processes: I know that the former are glial fibrillary acidic protein (GFAP)-positive glial cells including ependymal cells, and the latter are neurons (see Watanabe *et al*., 2006). On the other hand, the α1 subunit of Na^+/K^+-ATPase was expressed in both cell types, expectedly (Fig. II.6E).

Because the α2 and α3 isoforms of the α subunit of Na^+/K^+-ATPase are also expressed in the nervous system (Shamraj and Lingrel, 1994), I subsequently examined the interaction of the α2 and α3 isoforms with the C-terminal region of Na_x. Experiments using the yeast two-hybrid system showed that the cytoplasmic fragment of α2 corresponding to the region of the α1 isoform isolated (amino acids: 593–714, Fig. II.1B) also interacted with the C-terminal region of Na_x, but that of α3 (586–707, Fig. II.1B) did not (Fig. II.7).

To know whether the three α subunit isoforms of Na^+/K^+-ATPase are coexpressed with Na_x channels in astrocytes and ependymal cells of the SFO, I performed *in situ* hybridization using adult mouse SFO tissue sections. The mRNAs encoding the α1 and α2 isoforms of Na^+/K^+-ATPase were expressed in the SFO with a similar pattern to the Na_x channels (Fig. II.8A–C). However, signals for the α3 isoform were not detected in the SFO (Fig. II.8D).

II.4 Discussion

In this chapter, I revealed that Na_x interacts with α subunit of Na^+/K^+-ATPase. The α subunit contains ATP catalytic domain and cation-binding sites for transporting function, and is often referred to as the catalytic subunit (Kaplan, 2002). There exist four isoforms of the α subunit (α1, α2, α3 and α4) with different tissue distributions. The α1, α2 and α3 isoforms of the α subunit of Na^+/K^+-ATPase are expressed in the nervous system (Shamraj and Lingrel, 1994). I showed that Na_x has specific interaction with α1 and α2 isoforms of the α subunit of Na^+/K^+-ATPase (Fig. II.7). The α1 and α2 isoforms are reportedly expressed in astrocytes (McGrail *et al*., 1991; Watts *et al*., 1991), consistent with the finding that the Na_x channel is expressed in glial cells in the CVOs (Watanabe *et al*., 2006). The expression of α1 and α2, but not α3, was detected in the SFO by *in situ* hybridization (Fig. II.8), suggesting the functional relevancy *in vivo*. Of note is that the amino acid sequence corresponding to the interacting region in the α3 isoform contains significant substitutions relative to the α1 and α2 isoforms (Fig. II.1B). The subunit specificity was functionally verified by coexpression experiments using the binding region of the α subunits (see Chapter III).

The Na^+/K^+-ATPase functions in almost all animals as the principal regulator of intracellular Na^+ and K^+ concentrations using ATP as an energy source. During each active cycle 3 Na^+ ions are pumped out of the cell in exchange for 2 incoming K^+ ions for every ATP molecule consumed (Sweadner, 1989, 1995). Cosequently, the ATP hydrolysis of Na^+/K^+-ATPase is considered to be enhanced when intracellular Na-level increases above usual level (Pellerin *et al*., 1998). This implies that Na_x, as a sodium channel, can upregulate Na^+/K^+-ATPase by supplying Na. The close interaction between Na_x and Na^+/K^+-ATPase, reveled in this chapter, further facilitated me to speculate that Na_x channels have a direct influence on molecular properties of the Na^+/K^+-ATPase. In the next section, this hypothesis is tested.

In this study, I generated cDNA library from mouse DRG, for neurons and non-myelinating Schwann cells in DRG highly express Na_x, though the physiological role of Na_x in these cells still be unexplained. I found several molecules as candidates of binding proteins of Na_x. However, I have not obtained any hints for the

physiological roles of Na_x in CNS from the properties of the candidate proteins other than Na^+/K^+-ATPase. It is well known that the results of two-hybrid screening can greatly be affected by the cDNA library used in the experiment. So, I am planning to perform novel two-hybrid screenings using the other cDNA libraries, expecting to find new Na_x-binding molecules other than those I have already found.

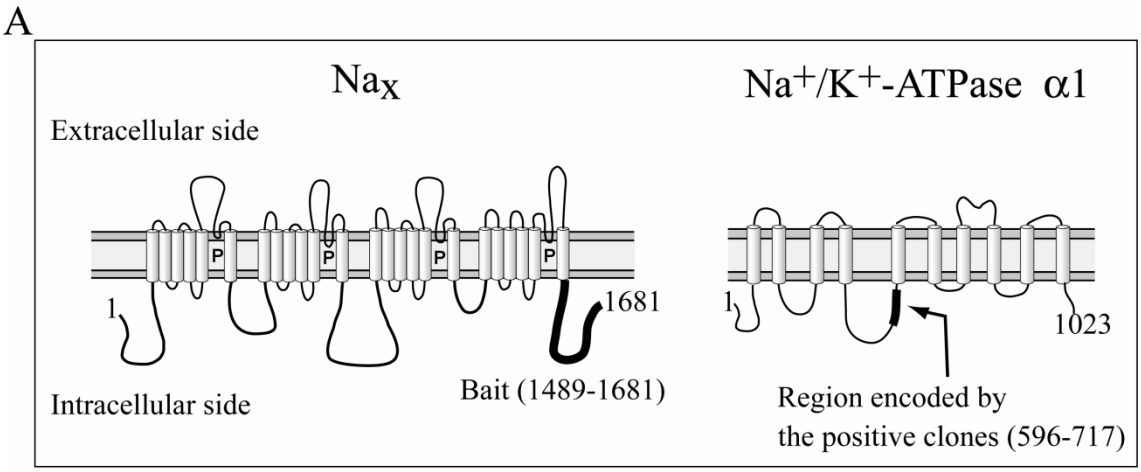

B

```
α1:596 RAAVPDAVGKCRSAGIKVIMVTGDHPITAKAIAKGVGIISEGNETVEDIAARLNIPVNQVN
α2:593 RAAVPDAVGKCRSAGIKVIMVTGDHPITAKAIAKGVGIISEGNETVEDIAARLNIPVSQVN
α3:586 RAAVPDAVGKCRSAGIKVIMVTGDHPITAKAIAKGVGIISEGNETVEDIAARLNIPVSQVN

α1:PRDAKACVVHGSDLKDMTSEELDDILRYHTEIVFARTSPQQKLIIVEGCQRQGAIVAVTGD 717
α2:PREAKACVVHGSDLKDMTSEQLDEILRDHTEIVFARTSPQQKLIIVEGCQRQGAIVAVTGD 714
α3:PRDAKACVIHGTDLKDFTSEQIDEILQNHTEIVFARTSPQQKLIIVEGCQRQGAIVAVTGD 707
```

Fig. II.1. Region in Na$_x$ used for two-hybrid experiments and region in Na$^+$/K$^+$-ATPase encoded by the positive clones.

(A) Schematic illustrations of Na$_x$ channel (Left) and α1 subunit of Na$^+$/K$^+$-ATPase (Right). The numbers represent amino acid residues. In Na$_x$, the C-terminal region of bold line represents a bait region used for the yeast two-hybrid screening. In the α1 subunit of Na$^+$/K$^+$-ATPase, the region encoded by the positive clones is drawn in bold. P, putative pore-forming regions.

(B) Alignment of amino acid sequences of the α1 (596–717), α2 (593–714) and α3 (586–707) isoforms of mouse Na$^+$/K$^+$-ATPase. Amino acids identical among them are shaded, and unique amino acids in α3 are drawn in red.

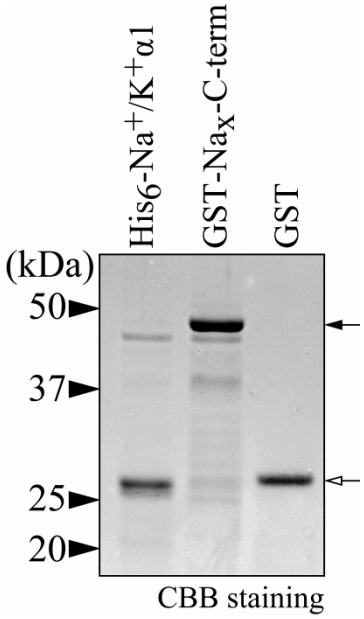

Fig. II.2. Purification of GST or His-tagged proteins for subsequent pull-down assays.

Purified proteins were visualized by CBB staining. Closed arrow indicates GST-Na_x-C-term (amino acid residues 1,489–1,681) at 47 kDa, open arrow indicates His_6-Na^+/K^+α1 fragment (amino acid residues 591–759 of the α1 subunit of Na^+/K^+-ATPase) at 26 kDa, and GST at 27 kDa.

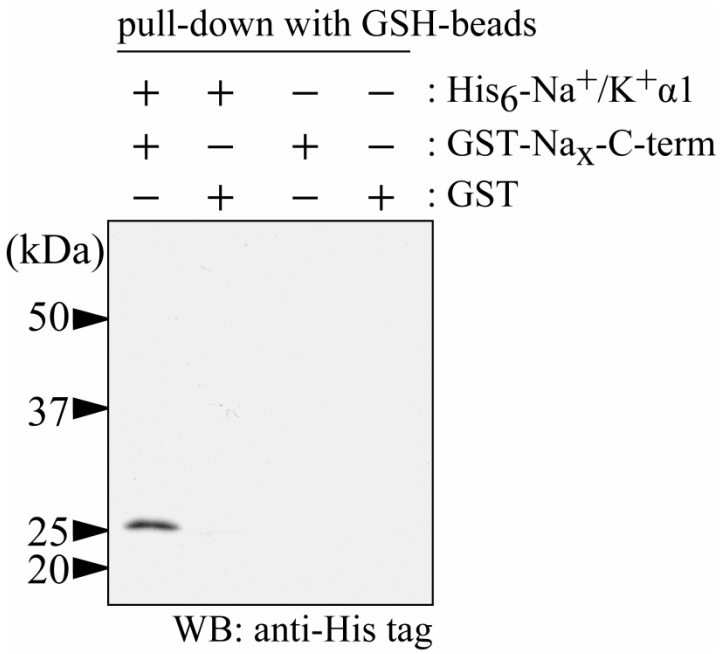

Fig. II.3. ***In vitro*** **binding assay between Na^+/K^+-ATPase and Na_x channels using purified proteins.**

Glutathione beads coated with GST-Na_x-C-term or GST were incubated with the purified His_6-Na^+/K^+α1 fragment. The bound His_6-Na^+/K^+α1 fragment was detected by Western blotting.

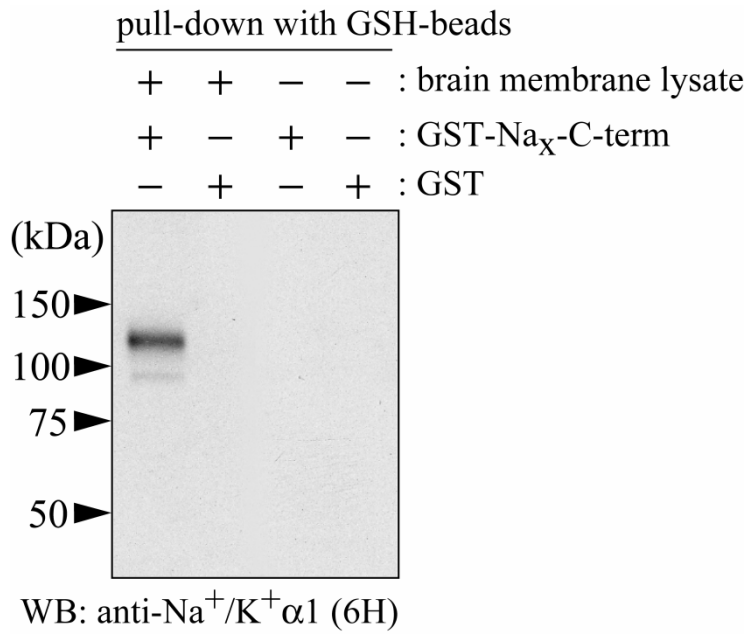

Fig. II.4. ***In vitro*** **binding assay between Na^+/K^+-ATPase and Na_x channels using brain membrane lysate.**

Glutathione beads coated with GST-Na_x-C-term or GST were incubated with the brain membrane lysate. The α1 subunit of Na^+/K^+-ATPase (Na^+/K^+α1) bound was detected by Western blotting.

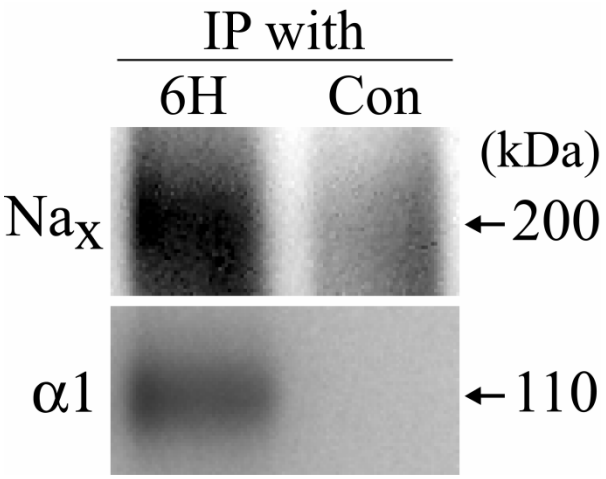

Fig. II.5. Coimmunoprecipitation of Na_x channels and the α1 subunit of Na^+/K^+-ATPase.

Cell lysate prepared from C6M16 cells was immunoprecipitated with a monoclonal antibody (6H) to the α1 subunit of Na^+/K^+-ATPase or anti-HA monoclonal antibody (Con) as a negative control, and analyzed by Western blotting using anti-Na_x antibody (upper) or 6H (lower).

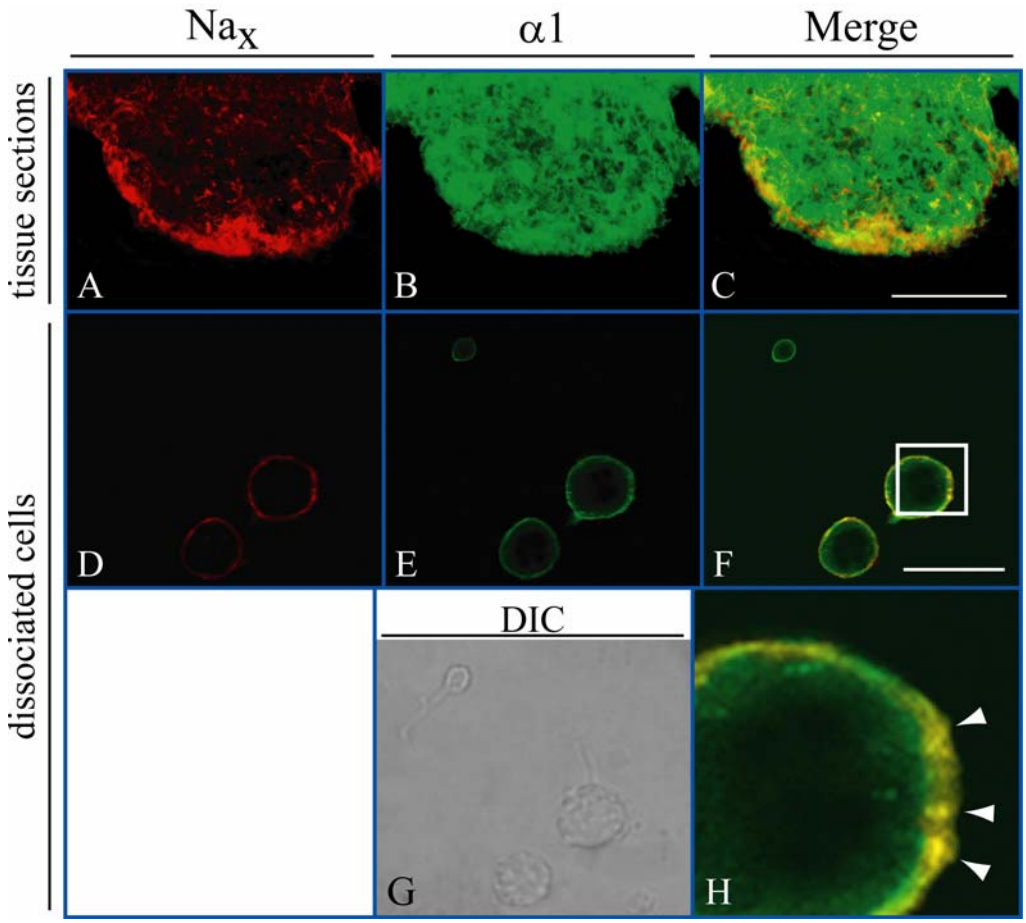

Fig. II.6. Colocalization of Na_x channels and the α1 subunit of Na^+/K^+-ATPase on coronal tissue sections and dissociated cells of the mouse SFO.

(A–H) Immunostaining of Na_x channels (Na_x) and the α1 subunit of Na^+/K^+-ATPase (α1) is merged to show the colocalization (Merge) for coronal tissue sections (A–C) and dissociated cells (D–H) of the mouse SFO. A higher magnified picture of the boxed area in (F) is shown in (H). Arrowheads in H point to the dense colocalization of Na_x and the α1 subunit in the plasma membrane. DIC, differential interference contrast image; scale bars: 100 μm for (A–C), 30 μm for (D–H).

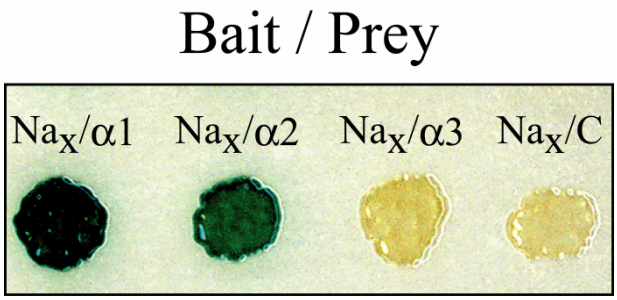

Fig. II.7. Filter-lift β-galactosidase assay to examine the binding of the C-terminal region of Na_x channels with the α1, α2 and α3 subunits of Na^+/K^+-ATPase.

The bait is the C-terminal region of Na_x. As prey, three polypeptides derived from the third cytoplasmic domain of the α subunit of Na^+/K^+-ATPase (shown in [Fig. II.1B]) were used (Na_x/α1–α3). As a negative control, only the GAL4-activating domain was expressed (Na_x/C).

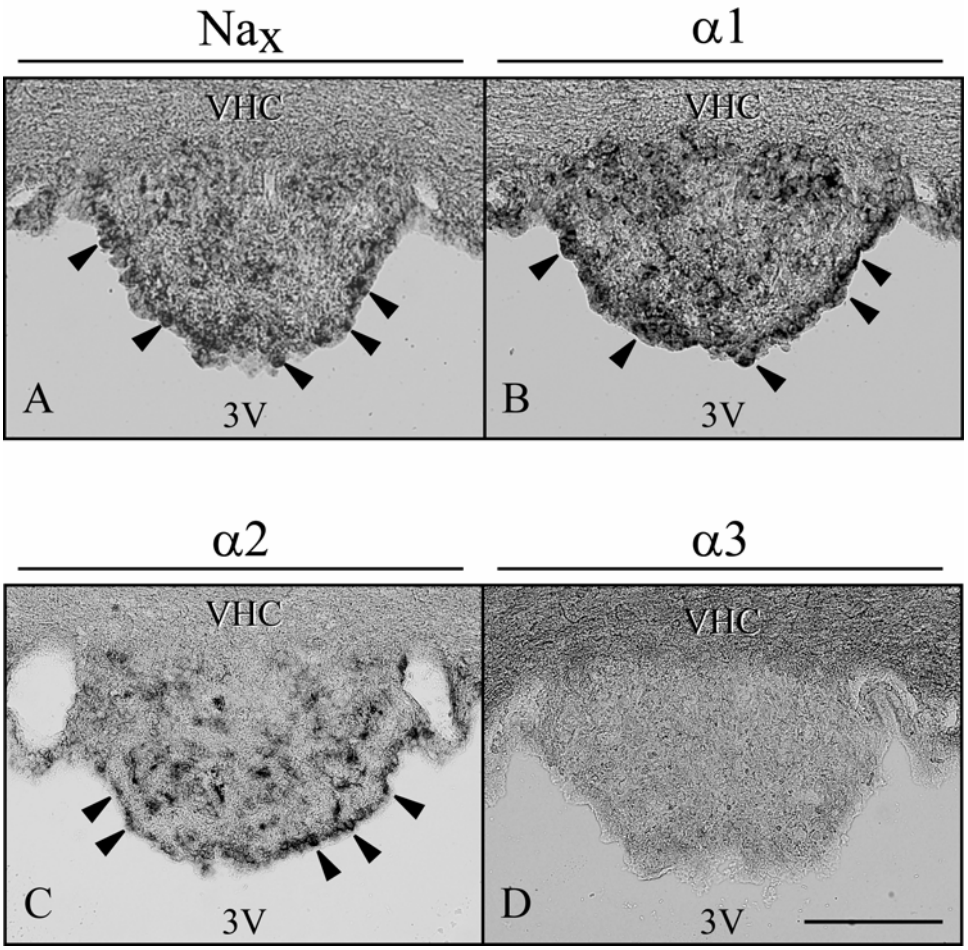

Fig. II.8. ***In situ*** **hybridization with probes for Na_x channel, and α1, α2 and α3 subunits of Na^+/K^+-ATPase on coronal tissue sections of the mouse SFO.**

The SFO is attached to the ventral hippocampal commissure (VHC) and faces the dorsal third ventricle (3V). Positive signals were observed in ependymal cells facing the 3V (arrowheads) and cells inside the SFO with the Na_x, α1, and α2 probes, but not with the α3 probe. Scale bar: 50 μm.

Chapter III

Functional coupling between Na_x channels and Na^+/K^+-ATPase, and Na^+ influx through Na_x on the bases of Na-dependent activities of glucose uptake in glial cells

III.1 Introduction

In Chapter II, I demonstrated that Na_x channels directly interact with α subunits of Na^+/K^+-ATPase. Na_x is a sodium channel, which opens in response to the elevation of extracellular Na^+ concentration and raises the intracellular Na^+ level. On the other hand, the activity of Na^+/K^+-ATPase can be regulated by Na^+ or K^+ balance between both sides of the plasma membrane (Kaplan, 2002). Thus it is probable that Na_x functionally regulates Na^+/K^+-ATPase by increasing Na^+ level in the cytoplasm. Furthermore, the close interaction of Na_x channels with the α subunits of Na^+/K^+-ATPase raised the notion that Na_x channels exert a direct influence on molecular properties of the Na^+/K^+-ATPase. If it was the case, cellular energy metabolism should be affected, because cells in the CNS use ~50% of their energy resources to drive the Na^+/K^+-ATPase activity (Rosenthal and Sick, 1992). In order to explore this possibility, I measured glucose uptake activity of the C6M16 cells by using a fluorescent glucose derivative, 2-NBDG (Yoshioka *et al*., 1996; Yamada *et al*., 2000): Rb^+, which is often used for measuring activities of Na^+/K^+-ATPase directly (Serpersu and Tsong, 1984), was not suitable in this case, because Rb^+ affects Na_x function (unpublished data). In this chapter, I first examined this idea using cell lines *in vitro*. However, attempts to establish stable cell lines expressing functional Na_x channels have been long unsuccessful. Therefore, I turned my attention to developing cell lines in which the expression of Na_x channel is inducible under the control of the tetracycline-responsive element (TRE). In this system, Na_x expression is induced by a transactivator, Tet-Off, which is secondly transfected and expressed with an adenoviral vector: It is possible to suppress the expression again in the presence of a tetracycline-analog, doxycycline (Dox), in this system established cell lines, in which Na_x expression is induced.

III.2 Materials and Methods

Establishment of Na_x-expressing C6 cells

The pTRE plasmid (Clontech) carries the Tetracycline-responsive element (TRE), which is under the control of the minimal immediate early promoter of cytomegalovirus, a multiple cloning site, and a SV40 polyA attachment sequence. A 6.1-kb $mNa_v2.3$ cDNA fragment including 0.3 kb of the 5' noncoding, 5.0 kb of the coding, and 0.8 kb of the 3' noncoding regions (GenBank accession number, L36179) was inserted into the multiple cloning site (pTRE-mNa_x). Plasmids pTRE-mNa_x and pKJ2 carrying the neomycin-resistance gene (Boer *et al*., 1990) were cotransfected into C6 rat glioma cells by lipofection (Lipofectamine, Invitrogen) according to the manufacturer's directions. The transfected C6 cells were selected in the presence of the neomycin-analog G418 (1.2 mg/ml, Invitrogen), and resistant cells were cloned by limiting dilution. For the selection of the positive clones, Na_x expression was induced as follows. C6 transformants were individually plated on culture dishes and incubated in DMEM containing 10% FCS under 5% CO_2 for 6 hr at 37°C. The medium was then changed to serum-free DMEM containing 1 mM N^6,2'-*O*-dibutyryl cyclic AMP (dbcAMP, Sigma), and the cells were further cultured for 36 hr at 37°C. For the induction of Na_x expression, the Tet-Off adenoviral vector (2.0×10^5 pfu, Clontech) was added to the medium. Expression of Na_x channels was checked by immunocytochemistry with anti-Na_x antibody as described previously (Hiyama *et al*., 2002). The expression of Na_x channels was detected by Western blotting as reported previously (Watanabe *et al*., 2000) to select four clones with high expression. One of the four clones was named C6M16 and mainly used for the present study. However, all the results obtained with C6M16 were reproduced using the other cell clones. The stable transformants were passaged in Dulbecco's Modified Eagle Medium (DMEM, Nissui Pharmaceutical, Tokyo, Japan) containing 10% fetal calf serum (FCS, Invitrogen).

Immunostaining of C6M16 cells

C6M16 cells cultured on collagen-coated glass coverslips were washed twice with PBS

and fixed in ice-cold methanol for 1 hr. Fixed cells were permeabilized with 0.04 % NP-40 in PBS for 20 min, and then blocked with 4% skim milk in PBS (blocking buffer). The cells were incubated overnight at 4°C with a mixture of primary antibodies in the blocking buffer and washed four times with PBS. To detect the binding of specific antibodies, cells were incubated for 1 hr with fluorescent dye-conjugated antibodies, and washed four times with PBS. Cells were mounted with Permafluor (Beckman Coulter Co., Marseille, France) and observed using a Zeiss LSM510 confocal microscope (Carl Zeiss, Jena, German). To quantify the colocalization of fluorescent signals, I calculated Pearson's correlation coefficient (*r*) by using the "colocalization finder" plug-in of ImageJ free software (National Institutes of Health, Bethesda; http://rsb.info.nih.gov/ij/).

Coexpression of the C-terminal region of Na_x or the Na_x-interacting region of the α subunits of Na^+/K^+-ATPase

The cDNA fragment of the Na_x-binding region of mouse Na^+/K^+-ATPase α1, α2, or α3 was inserted into the multiple cloning site of the pcDNA3.1 expression vector (Invitrogen). The C-terminal region of mouse Na_x (nucleotides 4,716–5,327) was inserted into the multiple cloning site of the pcDNA3.1/myc vector to express it with a myc-tag at the N-terminus. Plasmids were introduced into rat glioma C6M16 cells by electroporation with nucleofector II (Amaxa, Gaithersburg, MD) according to the manufacturer's directions. Six hours after the transfection, the expression of *Na_x* was induced as described above. In experiments shown in Fig. III.7, *Na_x* expression was not induced.

Na-ion imaging

C6M16 cells (1.0×10^4) were plated on polyethylenimine (Sigma) -coated glass-bottom dish (Matsunami Glass) and incubated in DMEM containing 10% FCS for 6 hr at 37°C. The medium was then changed to serum-free DMEM containing 1 mM dbcAMP. The expression of Na_x was induced as described above. Na-ion imaging was performed as described previously (Hiyama *et al*., 2002; Watanabe *et al*., 2006): Briefly, cells were loaded in advance with 4 μM Sodium-binding benzofuran isophthalate acetoxymethyl

ester (SBFI/AM, Molecular Probes) plus 0.02% Pluronic F127 (Sigma) for 15 min at 37˚C. During the recording, cells were continuously perfused at 1 ml/min with an isotonic solution containing (in mM): 135 NaCl, 5 KCl, 2.5 $CaCl_2$ 1 $MgCl_2$, 20 HEPES, and 10 NaOH, titrated to pH 7.3 with HCl (145 mM Na solution). Ten minutes after the start of the recording, the extracellular Na concentration was increased to 170 mM by replacing the perfusion solution with additional NaCl (170 mM Na solution). In some experiments, the Na ionophore monensin at a concentration of 0.5, 1, 2 or 5 μM was added to the 170 mM solution. The fluorescent ratio was monitored at excitation wavelengths of 340 and 380 nm using a microscope equipped with a cooled charge coupled device (CCD) camera (HiSCA, Hamamatsu Photonics, Hamamatsu, Japan). Data were collected every 30 s and analyzed using an image-analysis software (AQUACOSMOS version 2.5, Hamamatsu Photonics). After the recording, cells were fixed with a 10% formalin solution for 60 min at room temperature and subjected to immunostaining with anti-Na_x antibody.

Glucose imaging of C6 cells

For glucose imaging of C6 cells, the cells (1.0×10^4) were put onto polyethylenimine-coated glass-bottom dish and incubated in DMEM containing 10% FCS for 6 hr at 37°C. The medium was then changed to serum-free DMEM containing 1 mM dbcAMP. The expression of Na_x was induced as described above.

Glucose imaging was performed as described (Yoshioka *et al*., 1996). Briefly, cells were incubated containing 500 μM 2-(*N*-(7-nitrobenz-2-oxa-1,3-diazol-4-yl)amino)-2deoxyglucose (2-NBDG, Molecular Probes) for 10 min or 20 min at 37°C. After the application of 2-NBDG in the 170 mM Na solution at 37°C, the fluorescence intensity of the cell was gradually increased in proportion to the time at least until 30 min. In some experiments, the Na ionophore monensin (Sigma) at a concentration of 0.5, 1, 2 or 5 μM, or else 1 mM ouabain (Sigma) was added to the solutions. The cells were then washed five times with the 145 mM solution. Fluorescence of the cells and background was collected by a fluorescence microscope (IX71, Olympus) with barrier (wavelength 536 ± 40 nm, GFP-3035B,

Semrock, Rochester, NY) and excitation (wavelength 488 ± 10 nm, C7773, Hamamatsu Photonics) filters. Mean fluorescent intensities of cells were analyzed using the image-analysis software, and the average and standard error (SE) were calculated.

III.3 Results

Functional expression of Na_x in C6 cells

C6 is a rat glioma cell line devoid of endogenous *Na_x* expression (Gautron *et al*., 1992). I established four such inducible cell lines from C6 cells by transfection of an expression vector for *Na_x*. Fig. III.1A–III.1C show characteristic features of one of the four cell lines, C6M16. The expression of Na_x proteins began to be detected 24 hr after the viral transfection of the Tet-Off activator (Fig. III.1A, lane 2). The expression was completely inhibited with Dox at a concentration of 10 ng/ml or more (Fig. III.1A, lane 4). Immunocytochemistry with anti-Na_x channel antibodies confirmed these results (Fig. III.1B): Intensive immuno-positive signals were observed in the plasma membrane of the cells only when the expression of *Na_x* was induced (Fig. III.1Bb). Colocalization of the α1 subunit of Na^+/K^+-ATPase and Na_x channels at the subcellular level was observed in C6M16 cells by double-fluorescent immunocytochemistry (Fig. III.2, 145 mM).

By using an intracellular Na ion-imaging technique, our laboratory recently demonstrated that Na_x-positive cells dissociated from the SFO specifically show Na^+ influx in response to an increase of the extracellular Na level above the physiological level (Hiyama *et al*., 2002; Noda and Hiyama, 2005; Watanabe *et al*., 2006). In the present study, I examined whether the Na_x-expressing C6M16 cells acquired such Na-sensitivity using the same method. As shown in Fig. III.1C, C6M16 cells showed significant Na^+ influx in response to an increase in the extracellular Na level within the physiological range (from 145 mM to 170 mM) specifically under the conditions where Na_x channels are expressed. The results clearly indicated that functional Na_x channels were expressed in C6M16 cells through induction by Tet-Off. Similar results were obtained with the other three C6 lines (data not shown).

Colocalization of Na_x and the α1 subunit of Na^+/K^+-ATPase was confirmed by double-fluorescent immunostaining in C6M16 cells (Fig. III.2). The confocal microscopic analyses showed that both Na_x and α1 subunit were colocalized in the plasma membrane. The subcellular distribution and colocalization of the α1 subunit

and Na_x was not changed within 30 min when the extracellular Na concentration was increased from 145 mM to 170 mM at the level of light-microscopic resolution: The mean of Pearsons's *r* (± SE) = 0.65 ± 0.074 at 145 mM (n = 3); 0.65 ± 0.086 at 170 mM (n = 3).

Coupling between Na_x channels and Na^+/K^+-ATPase is the basis of the Na-dependent metabolic enhancement of the cells

C6M16 cells 36 hr after the viral transfection with or without the Tet-Off transactivator were used for the analysis (Fig. III.3A). The C6M16 cells did not show significant uptake of 2-NBDG in the 145 mM solution when the expression of Na_x was not induced (Con). In contrast, upon the expression of Na_x (Na_x), the cells showed substantial increase in 2-NBDG uptake in the 145 mM solution (Fig. III.3B, Na_x in 145 mM of C6M16). However, the enhancement was ouabain insensitive, indicating that it is independent of the Na^+/K^+-ATPase activity (compare Na_x with and without Ouabain in 145 mM of C6M16 cells). Here, it should be noted that this substantial 2-NBDG uptake in C6M16 cells in the 145 mM Na solution is not observed in the native cells (see below and Fig. IV.2).

I then compared the cellular activities of 2-NBDG uptake in isotonic (145 mM) and hypertonic (170 mM) Na solutions. The C6M16 cells with Na_x expression (Na_x) showed approximately 1.6-fold greater activity for 2-NBDG uptake in the 170 mM Na solution as compared with in the 145 mM solution ($p < 0.05$), while the uptake by the C6M16 cells without Na_x expression (Con) was not increased in the 170 mM Na solution (Fig. III.3, Con in 170 mM in C6M16). The increase in the uptake of 2-NBDG in Na_x-expressing cells in the 170 mM Na solution was completely inhibited by 1 mM ouabain (Fig. III.3B), indicating that the activity of Na^+/K^+-ATPase plays an essential role in the glucose demand induced by the elevation of the extracellular Na level.

Next, I tested the effect of overexpression of the Na_x-binding fragments (Fig. II.1B) of α1 and α2 subunits of Na^+/K^+-ATPase in C6M16 cells, because these fragments are expected to work as a competitor of Na^+/K^+-ATPase for binding to Na_x channels. As was expected, the transfection of an expression vector carrying the fragments of the

α1 and α2 subunits significantly suppressed the metabolic response in the C6M16 cells with Na_x expression in the 170 mM Na solution (Fig. III.4; $p < 0.05$). In contrast, overexpression of the fragment of the α3 subunit, which was negative for interaction with Na_x channel (see Fig. II.7), did not suppress the metabolic activation (Fig. III.4).

The C-terminal fragment of Na_x was also expected to work as a competitor for the binding of Na_x channels to Na^+/K^+-ATPase. Unexpectedly but intriguingly, overexpression of the C-terminal fragment of Na_x further enhanced the 2-NBDG uptake, when it was coexpressed in Na_x-positive cells (Fig. III.5, Na_x; $p < 0.05$). This suggests that the C-terminal region of Na_x is also able to support Na^+/K^+-ATPase, as well as the native Na_x. However, the expression of the C-terminal fragment of Na_x by itself (without concomitant expression of the native Na_x) exerted no effect on the 2-NBDG uptake (Fig. III.5, Con). This strongly suggests that a function of the native Na_x channel (presumably Na^+-influx activity) is also essential for the upregulation of the metabolic state, in addition to the function which is substitutable with the C-terminal region of Na_x.

Na^+ influx is necessary but not sufficient for the metabolic activation

To estimate the contribution of Na^+ influx itself to the metabolic activation, I tested the effect of the influx generated by a Na-specific ionophore, monensin (Harootunian *et al*., 1989), on the uptake of glucose. Na-imaging experiments with C6M16 cells clearly showed that monensin induced Na^+ influx in a dose-dependent manner (Fig. III.6A): here, background fluorescence values in the cells without monensin were subtracted from respective values.

At a concentration of 0.5 μM, monensin triggered a small Na^+-influx into cells (Fig. III.6Ab) comparable to that of the C6M16 cells expressing Na_x when stimulated in the 170 mM solution (Fig. III.1C). However, the application of 0.5 μM monensin to C6M16 cells without Na_x-channel expression did not enhance the 2-NBDG uptake (compare Fig. III.6Ba and III.6Bb), and higher concentrations (2 and 5 μM) of monensin were not effective either (Fig. III.6Bc, 6Bd, and open bars in Fig. III.6C). In contrast, when Na_x-expressing cells were treated with 0.5, 2, and 5 μM monensin, the 2-NBDG

uptake was markedly enhanced dose-dependently (compare Fig. III.6Be and 6Bf, and filled bars in Fig. III.6C). This increase was not observed in the presence of ouabain (data not shown). These results clearly indicate that the increase of the Na-ion concentration in the cell is not enough by itself to trigger the uptake of glucose (metabolic stimulation), and that the presence of Na_x channel protein is required for the stimulation of glucose uptake by the cells.

Surprisingly and importantly, the C-terminal fragment of Na_x showed markedly enhanced 2-NBDG uptake under the condition without Na_x-channel expression with 0.5 μM monensin (Fig. III.7, Mon). The increase was cancelled out by the ouabain treatment (Fig. III.7, Mon + Oua). This indicates that the full-length Na_x channel can be replaced by the C-terminal fragment under the condition where Na^+ influx was secured by monensin. Taken together, it is probable that both pre-stimulation of Na^+/K^+-ATPase (by interaction with Na_x channels through the C-terminal region of Na_x) and Na^+ influx (through Na_x channels or monensin) are essential for the activation of the Na^+/K^+-ATPase and the cellular metabolic stimulation.

III.4 Discussion

In this chapter, I reveled functional coupling between Na_x and Na^+/K^+-ATPase, using newly established stable cell line that inducibly express Na_x. To estimate the activation level of Na^+/K^+-ATPase, I measured glucose-uptake activity using fluorescent glucose analogue. In my experiment, Na-dependent upregulation of glucose uptake was almost completely inhibited by a Na^+/K^+-ATPase inhibitor, ouabain (Fig. III.3B). So, my glucose imaging definitely reflect the hydrolysis activities of Na^+/K^+-ATPase as far as Na-dependent upregulation, though the mechanism of Na-independent enhancement (observed in Na_x comparing to Con in 145 mM of C6M16) still remains to be elucidated for future studies.

In the previous chapter, I reveled the isoform specificity of α subunits of Na^+/K^+-ATPase in the interaction to Na_x. In Fig. III.4, the specificity was functionally verified by coexpression experiments using the Na_x-interacting region of α subunits of Na^+/K^+-ATPase: the fragment of the α1 and α2 isoforms showed dominant negative activity on the glucose-uptake activity, but not that of α3. The specific interaction between Na_x and Na^+/K^+-ATPase thus appears to be indispensable for the upregulation of glucose uptake.

On the other hand, when the C-terminal fragment of Na_x was overexpressed in the Na_x-positive C6M16 cells, the Na-dependent glucose-uptake were further enhanced (Fig. III.5). This indicates that some of the Na^+/K^+-ATPase was free of interaction with Na_x in the cell because of a shortage of Na_x, and overexpression of the C-terminal region stimulated this population of the enzyme. For the glucose-uptake stimulation of the cell by the C-terminal region, either coexpression of the native Na_x (Fig. III.5) or the application of monensin is requisite (Fig. III.7). This indicates that Na^+ influx is a requirement to set Na^+/K^+-ATPase in motion, inducing demand for glucose to supply ATP to Na^+/K^+-ATPase.

It has been believed that Na^+ influx is sufficient for the activation of Na^+/K^+-ATPase by itself (Pellerin *et al*., 1998). However, monensin treatments alone, which induces extensive Na^+ influx (Fig. III.6A), had little effect on the Na^+/K^+-ATPase-dependent glucose-uptake in Na_x-negative cells (Con in Fig. III.6C and III.7). Only when the C-terminal fragment of Na_x (Fig. III.7, Na_x-C-term) or the

full-length Na_x (Fig. III.6C, Na_x) was coexpressed with Na^+/K^+-ATPase, did monensin induce substantial glucose uptake. Taken all together, it is probable that pre-activation (sensitization) of Na^+/K^+-ATPase occurs by the binding of Na_x and that this is essential for the Na dependent activation and drive of Na^+/K^+-ATPase. The direct binding between Na_x and Na^+/K^+-ATPase implies a favorable situation that Na ions flowed into the cell through Na_x are directly supplied to Na^+/K^+-ATPase.

Recently, several molecules, including nicotinic ACh receptor, FXYD1, FXYD 2, Src tyrosine kinases, and cofilin, were found to interact with Na^+/K^+-ATPase (Krivoi, *et al*., 2006; Feschenko *et al*., 2003; Zouzoulas and Blostein *et al*., 2006; Wang and Yu *et al*., 2005; Jung J, *et al*., 2002): Some reportedly activate or modify the properties of Na^+/K^+-ATPase through interaction. Here, cofilin is intriguing because it enhances Na^+/K^+-ATPase activity and binds triose-phosphate isomerase (TPI), a member of glycolytic pathway, suggesting of a direct coupling between the Na^+/K^+-ATPase and glycolytic activity (Jung J, *et al*., 2002). Of note is that clones encoding TPI were included in the positive clones in my yeast two-hybrid screening using the C-terminal region of Na_x as bait (unpublished observation).

In summary, in this chapter, I demonstrated that the glucose uptake of Na_x-expressing cells was markedly enhanced in response to an increase of the extracellular sodium concentration. It is probable that both prestimulation of Na^+/K^+-ATPase (by interaction with Na_x channels through the C-terminal region of Na_x) and Na^+ influx (through Na_x channels or monensin) are essential for the activation of the Na^+/K^+-ATPase and the cellular metabolic stimulation.

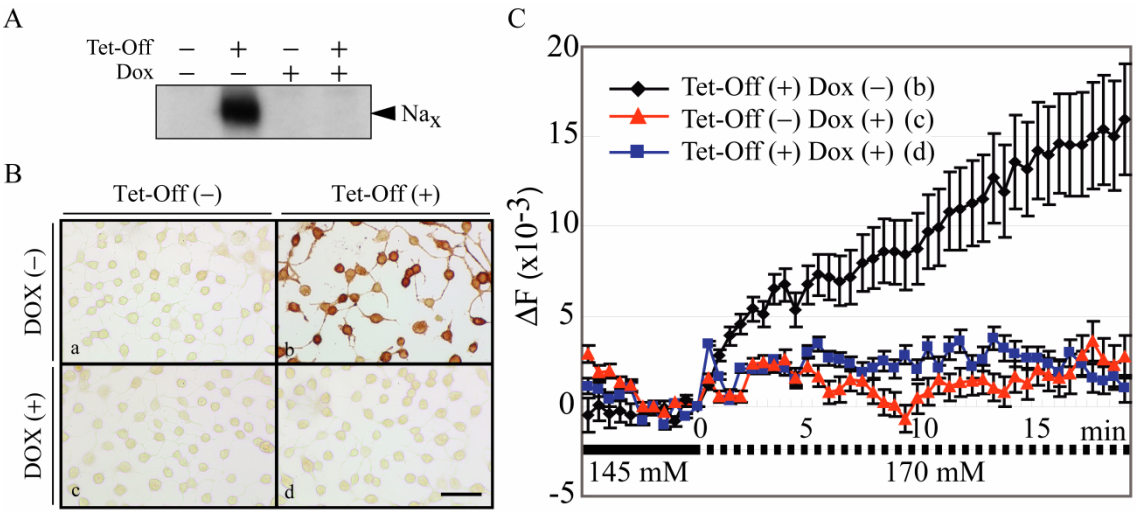

Fig. III.1. Functional expression of Na_x channels in rat C6 glioma cells.

(A) Western blotting with anti-Na_x antibody to examine the expression of Na_x channel protein in a cell line, C6M16, with (+) or without (–) the Tet-Off regulator. Na_x protein was observed only in the induced condition. The presence of doxycycline effectively suppressed the expression of Na_x channels.

(B) Immunostaining of Na_x channels expressed in C6M16. The Tet-Off regulator induces the expression of Na_x in the absence of doxycycline (Bb). Scale bar: 50 μm.

(C) Na imaging using SBFI in C6M16 cells in a high Na solution. The coordinate shows the fluorescent ratio (ΔF, 340 / 380 nm) representing the intracellular Na concentration. The fluorescent ratio at 0 min was set as zero points on the coordinate. Here, the continuous background increase by the host cell [Tet-Off(–) Dox(–)] was subtracted from respective values. The extracellular perfusion solution was changed from the 145 mM Na solution to the 170 mM Na solution at 0 min. Data are the mean and SE (n = 40 for each).

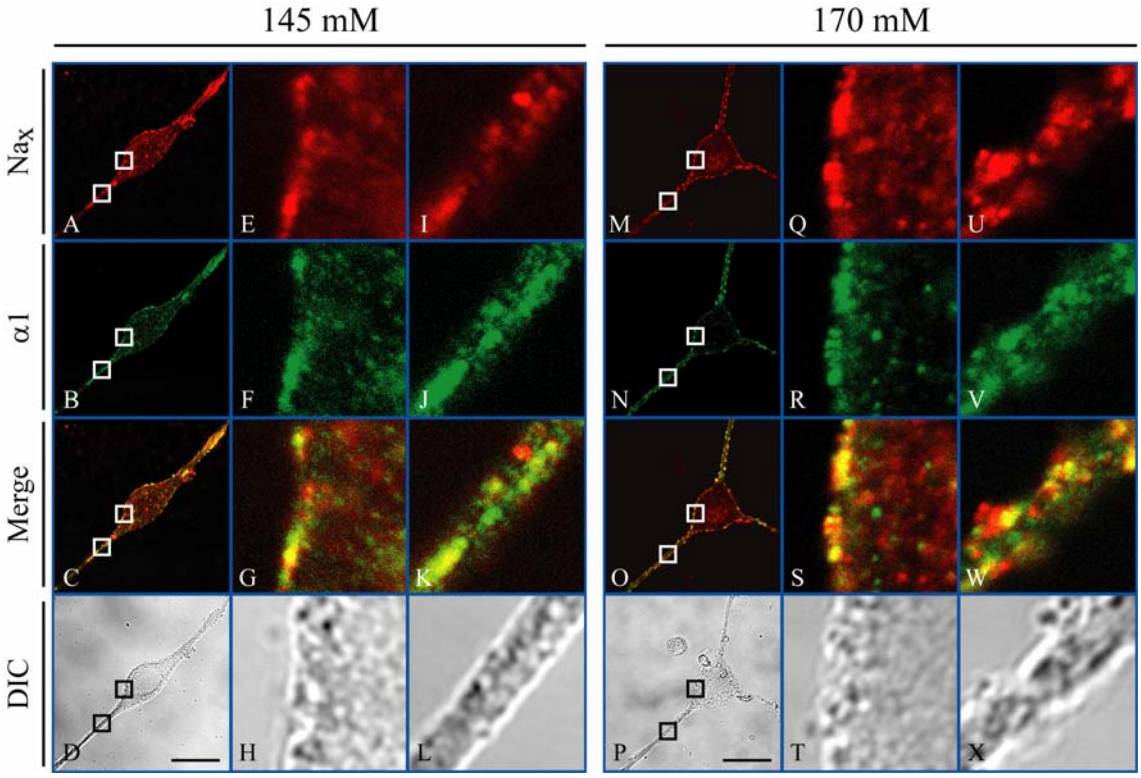

Fig. III.2. Colocalization of Na_x channels and α1 subunits of Na^+/K^+-ATPase in C6M16 cells.

Immunostaining of C6M16 cells expressing Na_x channels. Cells were incubated in a 145 mM or 170 mM Na solution for 30 min. The cells were immediately fixed, and double-stained as above. The panels of E–L and Q–X are higher magnifications of the boxed areas of A–D and M–P, respectively. Scale bars: 20 μm

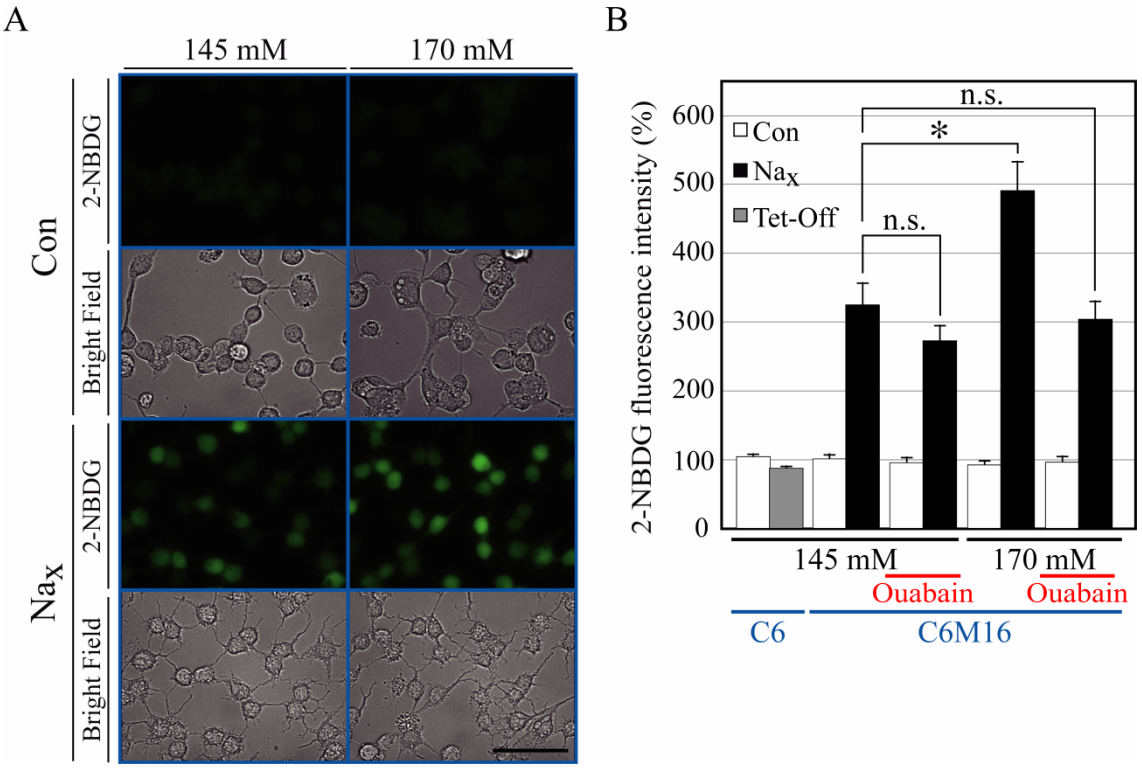

Fig. III.3. Interaction between Na_x and Na^+/K^+-ATPase is the basis for Na^+-dependent stimulation of the cellular glucose metabolism.

(A) Measurements of glucose-uptake activity of C6M16 cells. Only C6M16 cells expressing Na_x (Na_x) showed uptake of a fluorescent glucose derivative, 2-NBDG. Scale bar: 50 μm.

(B) Glucose-uptake activity of C6 and C6M16 cells in various conditions. An open bar and its neighboring shaded bar on the left end are data from the native C6 glioma cells (C6) non-transfected (Con) and transfected with the Tet-Off vector (Tet-Off), respectively. The other open and closed bars are data from C6M16 cells (C6M16) non-transfected (Con) and transfected with the Tet-Off (Na_x), respectively. In some experiments, 1 mM ouabain, a specific blocker of Na^+/K^+-ATPase, was applied (Ouabain). Fluorescent intensity of Con in the 145 mM of C6M16 was set at 100%. *$p < 0.05$, Bonferroni's multiple comparison test (against Na_x in 145 mM in C6M16); n.s., not significant; Data are the mean and SE (n = 40 for each).

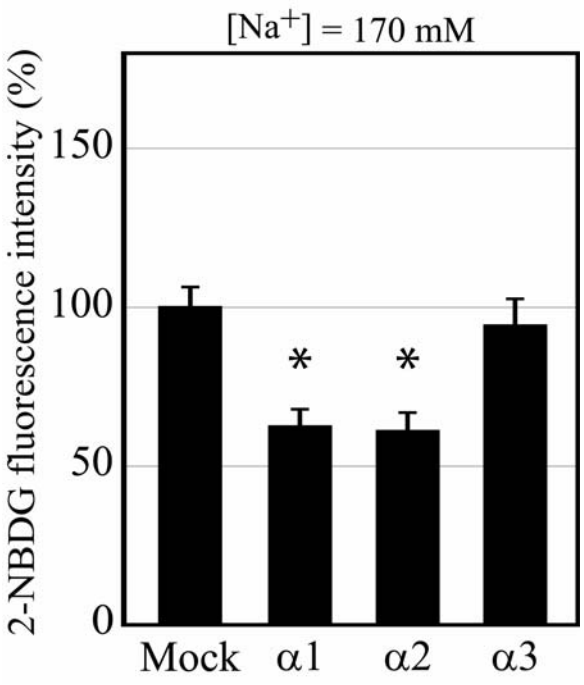

Fig. III.4. Glucose-uptake activity of the cells with coexpression of the Na_x-interacting region of respective α subunits of Na^+/K^+-ATPase in 170 mM Na solution.

2-NBDG uptake was significantly inhibited in Na_x-positive C6M16 cells by coexpression with the interacting regions of α1 and α2 subunits, but not of the α3 subunit, of Na^+/K^+-ATPase, compared with that in the cells transfected with the control pcDNA3.1 vector (Mock). All cells were transfected with the Tet-Off vector to induce Na_x expression, and subjected to 2-NBDG uptake assays in the 170 mM Na solution. Fluorescent intensity of the Mock condition was set at 100%. *$p < 0.05$, Bonferroni's multiple comparison test (against Mock); data are the mean and SE ($n = 40$ for each).

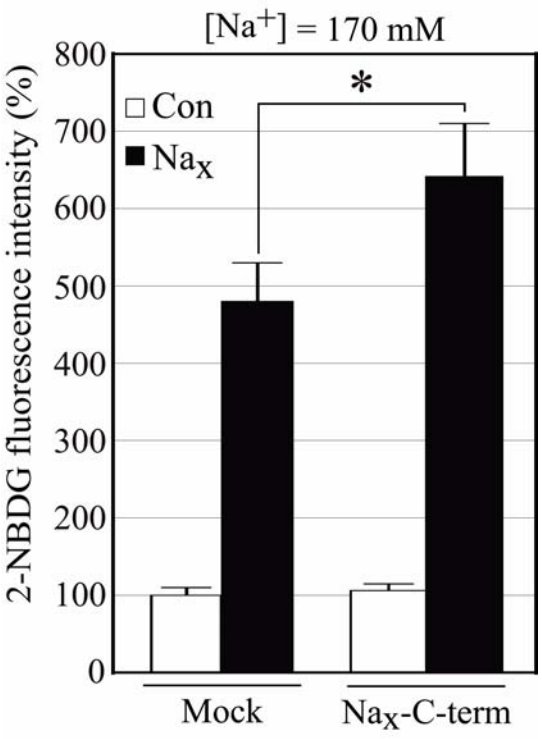

Fig. III.5. Glucose-uptake activity of the cells with coexpression of the C-terminal region of Na_x in 170 mM Na solution.

C6M16 cells were transfected with the expression vector for the C-terminal region of Na_x or control pcDNA3.1 vectors (Mock). Next, Na_x was not induced (Con, open bars) or induced (Na_x, closed bars) by the Tet-Off vector transfection and then used for 2-NBDG uptake assays in the 170 mM solution. The cellular fluorescent intensity of 2-NBDG was significantly enhanced in Na_x-positive C6M16 cells when transfected with the Na_x C-terminal region, compared with the cells transfected with the control vector. In Na_x-negative C6M16 cells, no such enhancement by the C-terminal of Na_x was observed. Fluorescent intensity of Con of the Mock condition was set at 100%. *$p < 0.05$, two-tailed t test (against Na_x of Mock); data are the mean and SE (n = 40 for each).

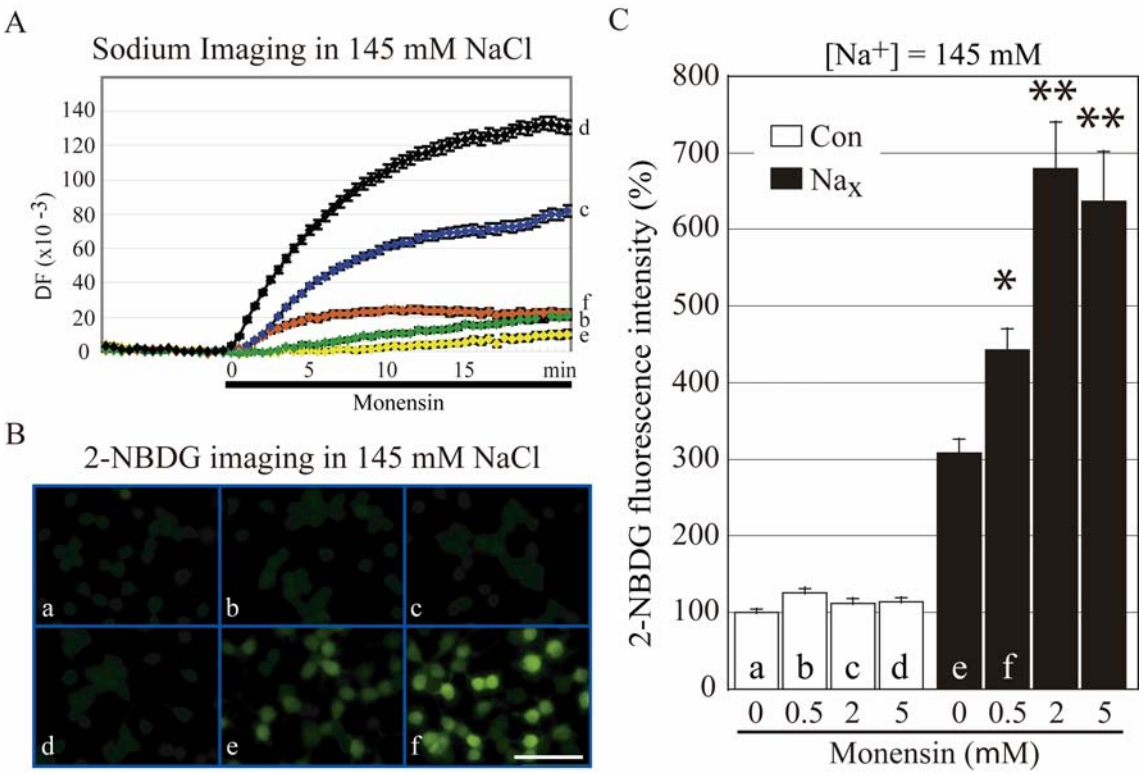

Fig. III.6. Activation of glucose uptake requires both Na^+ influx and stimulation of Na^+/K^+-ATPase by Na_x channels through the C-terminal region.

(A) Na^+ influx in C6M16 cells induced by monensin treatment. The coordinate gives the fluorescent ratio (ΔF, 340 / 380 nm) of SBFI, representing the intracellular Na concentration. The fluorescent ratio at 0 min was set as zero. The experimental conditions for (a–f) are common to (A–C): Na_x-noninduced cells (a–d), Na_x-induced cells (e and f). The 145 mM Na solution was changed to a monensin-containing 145 mM solution at 0 min; 0 μM (Ae), 0.5 μM (Ab and Af), 2 μM (Ac) or 5 μM (Ad). Background fluorescence values of Na_x-negative cells without monensin (see Ba) were subtracted from respective values. Data represent the mean and SE (n = 40 for each). (B) Fluorescent images 10 min after 2-NBDG loading in 145 mM Na solutions containing monensin; 0 μM (Ba and Be), 0.5 μM (Bb and Bf), 2 μM (Bc) and 5 μM (Bd). Only Na_x-positive cells (Be and Bf) show significantly higher glucose uptake. Scale bar: 50 μm.

(C) Summary of the glucose imaging experiments. The Na ionophore monensin markedly enhanced the glucose uptake of Na_x-expressing cells (Na_x) but not Na_x-negative cells (Con). The lower-case characters (a–f) in the bars represent respective experimental conditions common to those in B. *$p < 0.05$ and **$p < 0.01$, Bonferroni's multiple comparison test (against 0 μM of Na_x); data are the mean and SE.

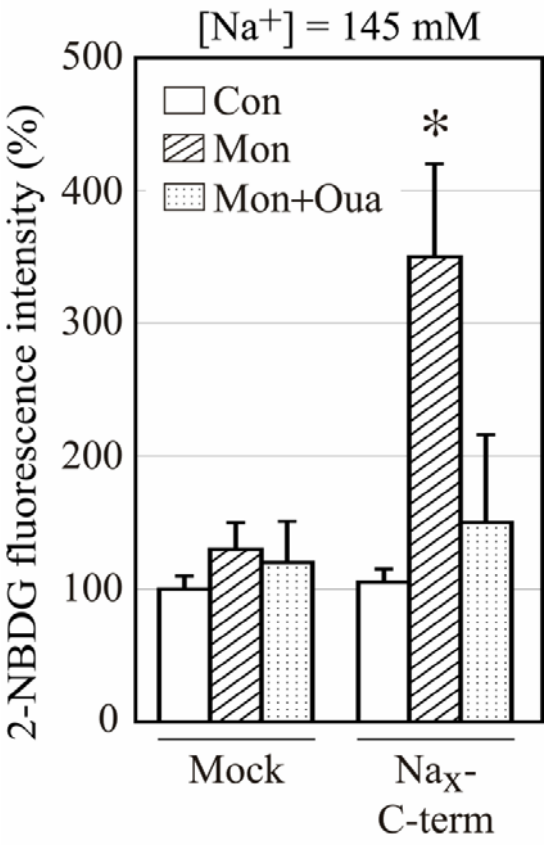

Fig. III.7. The role of the C-terminal region of Na_x in stimulating glucose metabolism.

The C-terminal region of Na_x (Na_x-C-term) or the control pcDNA3.1 vector (Mock) was transfected to C6M16 cells, and the cells were subjected to a 2-NBDG assay with 0.5 μM monensin (Mon), or 0.5 μM monensin and 1 mM ouabain (Mon + Oua) in the 145 mM Na solution. The mean fluorescence intensity of Con (without Mon or Oua treatment) of Mock was set at 100%. Note that the expression of Na_x channels was not induced in this experiment. *$p < 0.05$, Bonferroni's multiple comparison test (against Mon of Mock); data are the mean and SE (n = 40 for each).

Chapter IV

An increase of the extracellular Na concentration sensed by Na_x in glial cells is transmitted to neurons by lactate to activate neural activities of the SFO

IV.1 Introduction

In Chapter IV, I revealed that Na-level-dependent Na^+ influx through Na_x and direct interaction between Na_x and Na^+/K^+-ATPase leads to the activation of Na^+/K^+-ATPase in the C6 glioma cells. In this chapter, I examined whether the Na_x channel is actually involved in the energy control system in the Na_x-positive glial cells *in vivo*. I performed glucose-imaging analysis in the SFO, where specific glial cells expressing Na_x are located (Watanabe *et al*., 2006). I next examined the metabolic activity using another parameter. It is known that activation of anaerobic glycolysis leads to the production of lactate (Gladden, 2004). I measured the amounts of lactate and pyruvate released from the SFO to compare the results with those from imaging studies.

The conventional view that glucose oxidation fuels most activity-associated energy metabolism in neurons has recently been challenged by the astrocyte-neuron lactate shuttle hypothesis (Pellerin *et al*., 1998; Sibson *et al*., 1998; Magistretti, 2000), in which glial-produced lactate fuels neurons (Chih *et al*., 2001). Our laboratory has revealed that neurons in the SFO of *Na$_x$*-KO mice are hyperactivated under dehydrated conditions compared with wild-type mice (Watanabe *et al*., 2000) and that GABAergic neurons, which uses γ-aminobutyric acid (GABA) as a transmitter for the synaptic output, are one of the major neuronal types surrounded by Na_x-positive glial processes in the SFO (Watanabe *et al*., 2006). In this chapter, I then examined the neuronal activity of GABAergic neurons in the SFO under the high Na condition and the high lactate condition. I show that anaerobic glucose metabolism in the glial cells in the SFO is stimulated by Na-increase in the extracellular fluid. The resultant lactate released from the glial cells appeared to upregulate the firing activities of the GABAergic neurons in the SFO. Finally, I examined the mechanism of activation of neurons by lactate.

IV.2 Materials and Methods

Experimental animals

All the experiments with animals were carried out according to the guidelines of the National Institute for Basic Biology (Okazaki, Japan). Male wild-type (C57BL/6J, CLEA Japan, Tokyo, Japan), homozygous Na_x-gene knockout (Na_x-KO), heterozygous *GAD67-GFP* (Δ*neo*) knock-in (*GAD-GFP*), or *GAD-GFP* on the Na_x-KO genetic background (*GAD-GFP*/Na_x-KO) mice (Watanabe *et al*., 2006) at 8–24 weeks of age were used for experiments. All mice were housed in plastic cages under a constant room temperature (23˚C) with a 12 hr light/dark cycle (incandescent lights on at 7:00 A.M.). They were kept in this condition with *ad libitum* access to water and food (0.32% Na/Rodent Diet CE-2; CLEA Japan).

Pharmacological drugs

Among the drugs used in the experiments, DL-*threo*-β-Benzyloxaspartic acid (TBOA), 1,2,5,6-Tetrahydro-1-[2-[[(dyphenylmethylene)amino]oxy]ethyl]-3-pyridinecarboxylic acid hydrochloride (NNC711), β-alanine, 1-[2-[*tris*(4-methoxyphenyl)methoxy]ethyl]-(*S*)-3-piperidinecarboxylic acid (SNAP5114), 2,3-Dioxo-6-nitro-1,2,3,4-tetrahydrobenzo[f]quinoxaline-7-sulfonamide (NBQX), D-(–)-2-amino-5-phosphonopentanoic acid (APV), and tetrodotoxin (TTX) were purchased from Tocris (Bristol, UK). Apyrase, suramin, and diazoxide were from Sigma (St. Louis, MO).

Glucose imaging of SFO cells

For glucose imaging of SFO cells, the cells obtained as above were used (See Chapter II Materials and Methods). Glucose imaging was performed as described (Yoshioka *et al*., 1996). Briefly, cells were incubated containing 500 μM 2-NBDG (Molecular Probes) for 10 min or 20 min at 37°C. After the application of 2-NBDG in the 170 mM Na solution at 37°C, the fluorescence intensity of the cell was gradually increased in

proportion to the time at least until 30 min. In some experiments, the Na ionophore monensin (Sigma) at a concentration of 0.5 μM, or else 1 mM ouabain (Sigma) was added to the solutions. The cells were then washed five times with the 145 mM solution. Fluorescence of the cells and background was collected by a fluorescence microscope (IX71, Olympus) with barrier (wavelength 536 ± 40 nm, GFP-3035B, Semrock, Rochester, NY) and excitation (wavelength 488 ± 10 nm, C7773, Hamamatsu Photonics) filters. Mean fluorescent intensities of cells were analyzed using the image-analysis software, and the average and standard error (SE) were calculated.

Glucose imaging of SFO slices

The brains were removed from wild-type (n = 5) and Na_x-KO (n = 5) mice and put in an ice-cold cutting solution equilibrated with 95% O_2 and 5% CO_2. The composition of the cutting solution was as follows (in mM): 234 sucrose, 2.5 KCl, 0.5 $CaCl_2$, 10 $MgSO_4$, 26 $NaHCO_3$, 1.25 NaH_2PO_4, and 11 glucose, pH 7.3. The brains were cut into 250-μm coronal sections in the ice-cold cutting solution using a microslicer (Leica Microsystems). The slices were immediately placed in a solution equilibrated with 95% O_2 and 5% CO_2, and incubated for 10 to 30 min at 25°C. The composition of the solution was (in mM): 117.7 NaCl, 2.5 KCl, 2 $CaCl_2$, 1 $MgCl_2$, 26 $NaHCO_3$, 1.3 NaH_2PO_4, 14.6 mannitol, and 11 glucose, pH 7.3. The portion corresponding to the SFO and fornix was cut out from the slices by cutting at the corpus callosum. The samples were moved into the 145 or 170 mM Na solution containing 2-NBDG (200 μM), and incubated for 1 hr at 37°C. The samples were then fixed with a formalin solution and washed with PBS for 24 hr at room temperature. Fluorescent images were taken with a disc confocal unit (DSU system, Olympus) attached to an upright microscope.

Determination of lactate and pyruvate concentrations

SFOs dissected from wild-type (n = 8) and Na_x-KO (n = 8) mice were divided into 3 parts and incubated in 0.5 ml of modified Ringer solution, containing 1 μM TTX, for 24 hr at 37°C. The solutions containing SFOs were centrifuged at 9,200 *g* for 5 min and the supernatants were used for measurements. Lactate and pyruvate concentrations of

the supernatants were measured by an enzyme assay using lactate or pyruvate oxidase, respectively (Asanuma *et al*., 1985).

Electrophysiology

The *GAD-GFP* or *GAD-GFP/Na_x*-KO mice (Watanabe *et al*., 2006) were deeply anesthetized with diethyl ether and decapitated. The brains were quickly removed and submerged for 5–10 min in an ice-cold sucrose Ringer solution containing (in mM): 260 sucrose, 2.5 KCl, 10 $MgSO_4$, 0.5 $CaCl_2$, 5 HEPES, 10 glucose, and 5 NaOH, bubbled with 100% O_2 (pH 7.3 with HCl). Then, slices of 250 μm thick, cut at an angle of 45 degrees to the coronal plane with a microslicer (VT-1000, Leica Microsystems), were pre-incubated at room temperature for more than 1 hr before recordings. The recordings were made in a modified Ringer solution containing (in mM): 140 NaCl, 2.5 KCl, 2 $CaCl_2$, 1 $MgCl_2$, 10 HEPES, 10 glucose, and 5 NaOH, bubbled with 100% O_2 (pH 7.3 with HCl). For experiments in the 160 mM Na condition, 15 mM NaCl was added to the modified Ringer solution.

Slices were mounted in a recording chamber on an upright microscope (BX51WI, Olympus) and continuously perfused with the modified Ringer solution. GFP-positive and -negative neurons were selected using fluorescent optics, and then a cell-attached configuration was obtained using bright field optics. The firing rate of the GABAergic neurons was obtained from the data of 10 min (for Na), or 5 min (for lactate) after the solution was changed. Membrane potential was recorded under current-clamp configuration of patch-clamp technique in the modified Ringer solution containing 1 μM TTX. Patch pipettes were prepared from borosilicate glass capillaries and filled with the modified Ringer solution. The resistance of the electrodes was 3–7 MΩ in the Ringer solutions. All recordings were performed at 33–36°C. Data were acquired by using an axopatch 200B patch-clamp amplifier and the software pCLAMP 8 and analyzed with the software Clampfit (Axon Instruments, Foster City, CA).

IV.3 Results

Na_x is involved in the Na-dependent enhancement of glucose uptake in the SFO

To examine whether the Na_x channel is indeed involved in the energy control system in the Na_x-positive glial cells *in vivo*, I performed an imaging analysis of the uptake of glucose in the SFO using 2-NBDG, where specific glial cells expressing Na_x are located (Watanabe *et al*., 2006). The SFO from wild-type and *Na*$_x$-KO mice was sectioned frontally at 250 μm, incubated with 2-NBDG (200 μM) in the 145 mM or 170 mM Na solution for 1 hr, and observed with a confocal fluorescence microscope. Na-sensitive 2-NBDG uptake was obviously detected selectively in the wild-type (Fig. IV.1Aa and 1Ab; Fig. IV.1B, $p < 0.01$) but not in *Na*$_x$-KO (Fig. IV.1Ac and 1Ad; Fig. IV.1B) tissues: in the wild-type SFO incubated with 2-NBDG in the 170 mM solution, an intensively labeled mesh-like structure became apparent (Fig. IV.1Ab), suggesting that fine glial processes in the SFO actively took up the fluorescent derivative of glucose. These results clearly indicate that the SFO tissue has activity to take up glucose in response to a Na-level increase, and the Na_x channel is an essential component for this mechanism. The enhancement of 2-NBDG uptake in the wild-type SFO under the high Na condition was completely abolished by 1 mM ouabain (Fig. IV.1Ae and 1Af; Fig. IV.1B). These results indicate that the activity of Na^+/K^+-ATPase is the origin of the cellular energy demand at the tissue level *in vivo*.

Next, I examined the dissociated cells from the SFO to confirm that the cells showing the enhancement of 2-NBDG uptake express Na_x channels. Cells isolated from the SFO were incubated with 2-NBDG in the 145 mM or 170 mM Na solution for 20 min to estimate the glucose-uptake activity in the cells. After that, cells were fixed and stained with anti-Na_x antibody or anti-GFAP antibody. To verify that the cells that intensively took up glucose are glial cells, cells dissociated from the SFO of wild-type mice were stained with an antibody for glial fibrillary acidic protein (GFAP) following the glucose imaging study. The average fluorescence intensities of 2-NBDG in the 170 mM Na solution was ~4 fold higher than those in the 145 mM solution among GFAP-positive cells in the following staining (Fig. IV.2A and IV.2B for summary; $p <$

0.05). Among GFAP negative cells, the average fluorescence intensities did not show significant difference between the cells in 145 mM and those in 170 mM Na. Among the wild-type cells, cellular populations that intensively took up 2-NBDG in the 170 mM solution were present, and these cells were all positive for Na_x (Fig. IV.3A and IV.3B) and GFAP (Fig. IV.2). These results clearly indicate that the Na_x channel is an essential component for the upregulation of energy demand in the SFO under the high Na condition, as observed in the C6M16 cells.

The effect of monensin in the Na_x-positive C6M16 cells was reproduced in the native cells (Fig. IV.4). Cells dissociated from the SFO of wild-type mice showed a markedly enhanced uptake of 2-NBDG in the presence of 0.5 μM monensin, while the same stimulation of the cells from *Na_x*-KO mice induced little enhancement of the uptake.

Na_x channels enhance lactate release from the SFO Na-dependently

Increased demand for glucose by cells means that cellular glycolysis is enhanced to yield lactate (or pyruvate). To confirm this view, I next measured the amounts of lactate and pyruvate released from the SFO as another parameter of the metabolic activity (Fig. IV.5). The SFO tissues removed from mice of both genotypes were incubated in a modified Ringer solution (containing 145 mM or 160 mM Na) at 37°C for 30 hr with tetrodotoxin (TTX) to reduce the influence of neuronal activities on the glial cells. The Ringer solutions contained 10 mM glucose and 0 mM lactate. After the incubation, lactate and pyruvate concentrations in the solutions were measured by enzyme assays using lactate oxidase and pyruvate oxidase, respectively. As was expected, the wild-type SFO showed an increase in lactate secretion by ~60% compared with the *Na_x*-KO SFO (Fig. IV.5A, $p < 0.05$), consistent with the increase of glucose uptake (Fig. IV.1.A and 1.B; WT). On the other hand, amounts of pyruvate released into the medium were 10-fold lower than those of lactate and did not differ under the two different conditions (Fig. IV.5B). This indicates that anaerobic glycolysis was stimulated in Na_x-positive glial cells of the SFO under the high Na condition.

Na activates GABAergic neurons in the SFO by a Na_x-dependent mechanism

Neurons in the SFO of *Na_x*-KO mice are hyperactivated under dehydrated conditions compared with wild-type mice (Watanabe *et al*., 2000), and GABAergic neurons are one of the major neuronal types surrounded by Na_x-positive glial processes in the SFO (Watanabe *et al*., 2006). Then I examined the neuronal activity of GABAergic neurons in the SFO under the high Na condition. I prepared acute slices containing the SFO from *GAD-GFP* mice and *GAD-GFP/Na_x*-KO (see Watanabe *et al*., 2006), and recorded the firing activity of the GABAergic neurons bearing the fluorescence of GFP as marker by using patch-clamp techniques in the cell-attached mode under a fluorescence microscope. The GABAergic neurons in the SFO of both wild-type and *Na_x*-KO mice showed spontaneous firing at a similar frequency (Fig. IV.6: 4.25 ± 0.38 Hz for wild-type; 4.21 ± 0.35 Hz for *Na_x*-KO) under the 145 mM Na condition. After the extracellular Na-concentration was raised to 160 mM, the firing frequency of the GABAergic neurons in the SFO of wild-type mice gradually increased to 7.40 ± 1.21 Hz (Fig. IV.6, $p < 0.05$), but that of *Na_x*-KO mice did not show a significant change (4.35 ± 0.34 Hz). In these electrophysiological experiments using tissue slices, I used 160 mM of Na, instead of the 170 mM used for C6M16 and dissociated cells. This Na concentration corresponds to mild conditions in the physiological range of the increase, because the Na concentration in the plasma increases by 5–10% during dehydration (Wakerley *et al*., 1978; Nose *et al*., 1992).

Besides the Na_x channel, Na-dependent transporters for neurotransmitters are also conceivably involved in the modulation of neuronal activities by glial cells (Masson *et al*., 1999). An increase in the extracellular Na level induces Na^+ influx via Na_x, and resultantly reduces the ionic gradients of Na across the plasma membrane of glial cells, because the intracellular Na level reaches to ~35 mM finally (Noda and Hiyama, 2005). This presumably stimulates or attenuates the activity of Na-dependent glutamate and GABA transporters in glial cells: Glial cells are known to express several Na-dependent transporters of neurotransmitters, such as Na-dependent glutamate transporters (EAAT1/GLAST and EAAT2/GLT-1) and GABA transporters (GAT1, 2, or 3) (Anderson and Swanson, 2000; Conti *et al*., 2004). I examined the contribution of these transporters to the Na-dependent regulation of neuronal activities of the

GABAergic neurons in the SFO. By making electrophysiological recordings, I tested the effect of 100 μM TBOA (an inhibitor for EAATs), 0.1 μM NNC711 (a specific inhibitor for GAT1), 100 μM β-alanine (a specific inhibitor for GAT1/2), and 25 μM SNAP5114 (a specific inhibitor for GAT2/3). None of the treatments have any significant effects on the Na-dependent increase in the firing rate of the GABAergic neurons in the SFO, suggesting that these transporters are not involved in the Na-dependent upregulation of the spontaneous firing (Fig. IV.7).

I next explored the possibility that the Na-induced upregulation of the firing rate of the GABAergic neurons is mediated by some glutamatergic neurons projecting onto the GABAergic neurons in the SFO. I examined the effects of antagonists of glutamate receptors including 25 μM NBQX (an antagonist for AMPA/Kainate receptors) or 50 μM APV (an antagonist for NMDA receptor) by the electrophysiological recordings. Neither NBQX nor APV affected the Na-dependent increase in the firing rate of the GABAergic neurons, suggesting that glutamatergic neurons are not involved in the stimulation of the GABAergic neurons in the SFO (Fig. IV.8).

Moreover, I also examined the contribution of purinergic signaling (Fields and Burnstock, 2006), which is reportedly used for glial-neuronal communication in several regions of the brain. Neither apyrase (an ATPase) nor suramin (an antagonist for P2 purinergic receptors) affected the Na-dependent enhancement of spontaneous firing, indicating that purinergic signaling is not involved either (Fig. IV.9).

The Na-dependent neural activation by glial cells is mediated by lactate through monocarboxylate transporters

Because metabolic activation leads to the release of lactate from Na_x-positive glial cells, I next checked the possibility that lactate mediates the signal from the glial cells to GABAergic neurons to control the SFO activity. When lactate was added at 1 mM to the perfusate, the firing frequency of GABAergic neurons in the SFO of both wild-type and *Na_x*-KO mice increased (8.23 ± 0.78 Hz for wild-type; 8.22 ± 0.85 Hz for *Na_x*-KO; $p < 0.05$) (Fig. IV.10 and IV.11, Lactate). Furthermore, when 1 mM of lactate was added under the high Na condition, no additive effect on the neuronal activity was observed

(8.91 ± 0.81 Hz for wild-type; 8.65 ± 0.85 Hz for Na_x-KO) (Fig. IV.11, Na + Lactate). These results strongly indicate that lactate and Na share a common pathway in the stimulation of GABAergic neurons in the SFO. Lactate was most effective at ~1 mM in promoting the firing rate, and at higher concentrations, the firing was rather suppressed (Fig. IV.12).

Lactate is known to be transported to the cytoplasmic side by monocarboxylate transporters (MCTs) and fuels the oxidative metabolism in neurons (Gladden 2004). So, I examined the effects of α-Cyano-4-hydroxycinnamic acid (α-CHCA), an inhibitor of MCTs. The neural activation induced by the Na-level increase was inhibited by 5 mM α-CHCA (5.41 ± 0.92 Hz for wild-type; 5.30 ± 0.92 Hz for Na_x-KO) (Fig. IV.11, Na + α-CHCA). These results clearly indicate that the Na-dependent stimulation of GABAergic neurons is largely mediated by MCTs.

I also examined the effect of the other metabolic monocarboxylates, pyruvate and acetate, both known to be transported by MCTs. When pyruvate was added at 1 mM to the perfusate, the firing frequency of GABAergic neurons in the SFO of both wild-type and Na_x-KO mice similarly increased (8.80 ± 0.42 Hz for wild-type; 8.61 ± 0.35 Hz for Na_x-KO; $p < 0.05$) (Fig. IV.11, Pyruvate). By contrast, when acetate was added at 1 mM to the perfusate, the firing frequency was not significantly changed in either genotype (4.45 ± 0.38 Hz for wild-type; 4.36 ± 0.35 Hz for Na_x-KO) (Fig. IV.11, Acetate).

I further explored the activation mechanism underlying the increase in the firing rate of the GABAergic neurons. The finding that lactate and pyruvate are equally effective suggests that the GABAergic neurons are energetically stimulated. I found that Na-dependent potentiation of the firing activity of the GABAergic neurons were reduced by 0.3 mM diazoxide, an opener of the ATP-sensitive K channel (Kir6.2 / K_{ATP} channel) (Fig. IV.13A): The K_{ATP} channel closes in response to the increase of intracellular ATP level and depolarizes the cell. So, I examined the membrane potential of the GABAergic neurons during the application of lactate or high Na solution (Fig. IV.13B). The membrane potential was depolarized by both lactate and Na, and the depolarization effect was expectedly reduced by 0.3 mM diazoxide. These data thus support my view that lactate serves as an energy substrate to up-regulate the firing

activity of the GABAergic neurons.

IV.4 Discussion

In this chapter, I tried to examined whether the results obtained in the C6 cells are reproduced and showed that enhancement of glucose-uptake under the high Na condition was reproducibly observed in the SFO (Fig. IV.1–4; WT, 170 mM). The metabolic enhancement was ouabain sensitive and dependent to Na_x expression, suggesting that the Na-dependent activation observed *in vitro* and *in vivo* are mediated by the same mechanism. Furthermore, monensin treatments induced substantial glucose uptake in the SFO cells of WT mice (WT in Fig. IV.4), but not those of *Na$_x$*-KO mice (KO in Fig. IV.4), supporting the view from the data *in vitro*: pre-activation of Na^+/K^+-ATPase by the binding of Na_x is essential for the Na dependent activation and drive of Na^+/K^+-ATPase.

It is known that activation of Na^+/K^+-ATPase leads to stimulation of anaerobic glycolysis which leads to the production of lactate (Gladden, 2004). When the Na concentration of the incubating solution was increased to 160 mM, the SFO tissues obtained from WT mice indeed exhibited an increase in the release of lactate by ~60%, but those from the *Na$_x$*-KO mice showed no increase (Fig. IV.5A). Taken together with glucose imaging data, these results support the view that Na_x mediates the activation of Na^+/K^+-ATPase Na-dependently and stimulates anaerobic glycolysis to generate ATP to fuel it. Na_x-positive glial cells in the SFO of WT mice thus likely release lactate at higher level, in proportion to the Na concentration in body fluids elevated under dehydrated conditions.

The previous studies on *Na$_x$*-KO mice demonstrated that the Na_x channel exerts inhibitory influences on neuronal activities in the SFO, as judged from Fos immunoreactivity during dehydration (Watanabe *et al*., 2000). Na_x channels are expressed on perineuronal glial processes enveloping some neuronal types including GABAergic neurons in the CVOs (Watanabe *et al*., 2006). Thus the glial cells appear to regulate neural activities in the dehydrated animals to control the Na-intake behavior.

In this study, I found that there exist specific GABAergic neurons autonomously firing at ~4 Hz in the SFO: When the cholera toxin B subunit was injected into the

paraventricular nucleus for retrograde labeling, a major projection site from the SFO, the labeled neurons did not overlap with the GABAergic neurons (unpublished data), suggesting that most or all of the GABAergic neurons in the SFO are presumably not projection neurons but interneurons. The synaptic transmissions are supposedly not involved in the spontaneous firing, because antagonists of glutamate receptors exerted no significant effects on the firing (Fig. IV.8). Consistently, some population of the neurons in the SFO reportedly showed properties of spontaneous firing even when they were isolated (Washburn *et al*., 2000). The presence of spontaneously firing cells at ~2 Hz in slices has been reported also in other brain regions: e.g. GABAergic stellate cells in the cerebellum and cholinergic neurons in the striatum (Kondo and Marty, 1998; Goldberg and Wilson, 2005).

The electrophysiological data showed that the hypertonic Na solution enhanced the firing activity of the GABAergic neurons of WT but not Na_x-KO mice (Fig. IV 6; Na, Fig. IV.11). More importantly, lactate enhanced the activity of the GABAergic neurons of both genotypes (Fig. IV.10; Fig. IV.11, Lactate). Coapplication of Na and lactate did not have an additive effect on the neuronal activity (Fig. IV.11, Na + Lactate), indicating that the action of Na was mediated by Na_x, and that the actions of Na and lactate share a common pathway to enhance the firing activity of GABAergic neurons. Because the enhancement of glucose uptake by an increase in the extracellular Na level was inhibited by α-CHCA, an inhibitor of MCTs (Fig. IV.11, Na + α-CHCA), MCTs, which transport monocarbonates including lactate, pyruvate, and acetate, likely mediate the effect by Na.

Pyruvate is an aerobic fuel for the tricarboxylic acid cycle and supposedly produced from lactate by lactate dehydrogenase 1 in neurons (Gladden, 2004). Pyruvate also had a stimulating effect on the GABAergic neurons *in vitro* (Fig. IV.11, Pyruvate). However, there were no differences in the release of pyruvate between the SFO of WT and KO mice, along with no increase dependent on the Na level (Fig. IV.5B). In contrast, acetate did not have any stimulating effect on the GABAergic neurons (Fig. IV. 11, Acetate). Based on these findings, I concluded that lactate is the substance signaling from glial cells to neurons to activate neural activity. Consistently, it is known that lactate is preferentially metabolized in neurons than astrocytes and acetate is specifically metabolized in astrocytes (Waniewski and Martin, 2004).

Lactate at 1–2 mM was most effective for the activation of GABAergic neurons, and higher concentrations of lactate actually suppressed the firing activities (Fig. IV.12). Because neurons have MCT2 with higher affinity (Km for lactate is ~0.7 mM), the rate of lactate-uptake was readily saturated at a few mM (Hertz and Dienel, 2004). On the other hand, astrocytes have low affinity transporters, MCT1 (Km for lactate is 3–5 mM) and MCT4 (Km is 15–30 mM), therefore, the rate of lactate-uptake rises with the lactate concentration (Hertz and Dienel, 2004). The mechanism of the repression in the GABAergic neurons with the higher concentration of lactate is left for future investigation.

According to the astrocyte-neuron lactate shuttle hypothesis (Pellerin *et al*., 1998; Sibson *et al*., 1998; Magistretti, 2000), in which glial-produced lactate fuels neurons (Chih *et al*., 2001), neural activity increases the extracellular concentration of glutamate or GABA, whose uptake by glia stimulates Na^+/K^+-ATPase and glutamine synthetase activity. This stimulates glial anaerobic glycolysis, the conversion of glucose to lactate. Glial cells release lactate, and neurons use it to fuel their activity. According to a model, ~70% of the total pyruvate/lactate that is oxidized in neurons is supplied from glial cells (Hyder *et al*., 2006). Moreover, it has been suggested that lactate becomes a major substrate for neurons during prolonged stimulation, because lactate increases above the base level (Hu *et al*., 1997). In the present study, I revealed that lactate is the major fuel in the GABAergic neurons in the SFO (Fig. IV.5A): The release of pyruvate was small and not regulated by the Na level (Fig. IV.5B). For extensive firing of neurons, the activity of the neuronal Na^+/K^+-ATPase must be kept at a high level to keep the ionic gradient across the neuronal membrane. There is the possibility that continuously-firing neurons like the GABAergic neurons in the SFO are more or less in an energy-deficient condition in a steady state. The lactate released from the Na_x-positive glial cells under dehydrated conditions must be specifically used as an energy source to replenish the GABAergic neurons to keep the Na^+/K^+-ATPase activity at a high level.

Here, it is possible that the effect of lactate is mediated by the K_{ATP} channel: Lactate stimulates the generation of ATP through aerobic metabolism in neurons, which is responsible for closing the channel and depolarization of the neurons (Song and Routh,

2005). The experimental data using diazoxide, an opener of the K_{ATP} channel, support the possibility that the K_{ATP} channel mediates the promotion of firing rate of the GABAergic neurons in the SFO (Fig. IV.13A). Consistently, the depolarization effect of lactate and Na in the GABAergic neuron was reduced by diazoxide (Fig. IV.13B). However, I cannot conclude at present that this is the sole mechanism for the stimulation of the GABAergic neurons in the SFO, because specific antagonists for K_{ATP} channel are not available. This is analogous to a recent finding that lactate is an alternate energy substrate to regulate neuronal activities of glucose-sensing neurons in the ventromedial hypothalamic nucleus (Song and Routh, 2005). However, it should be noted that lactate stimulated the GABAergic neurons in the presence of 10 mM glucose in my slice system.

Taken together the results in this chapter, I found that lactate is used for the signaling substance from Na_x-positive glial cells to neurons in Na-level sensing. I found Na-dependent increase of anaerobic metabolism of glucose by the glial cells in the SFO, which produces lactate as the end product. Electrophysiological data indicates that lactate released from Na_x-positive glial cells upregulate the firing rate of GABAergic neurons in the SFO. My data further suggest that depolarization mediated by K_{ATP} channels underlies the upregulation of the GABAergic neurons.

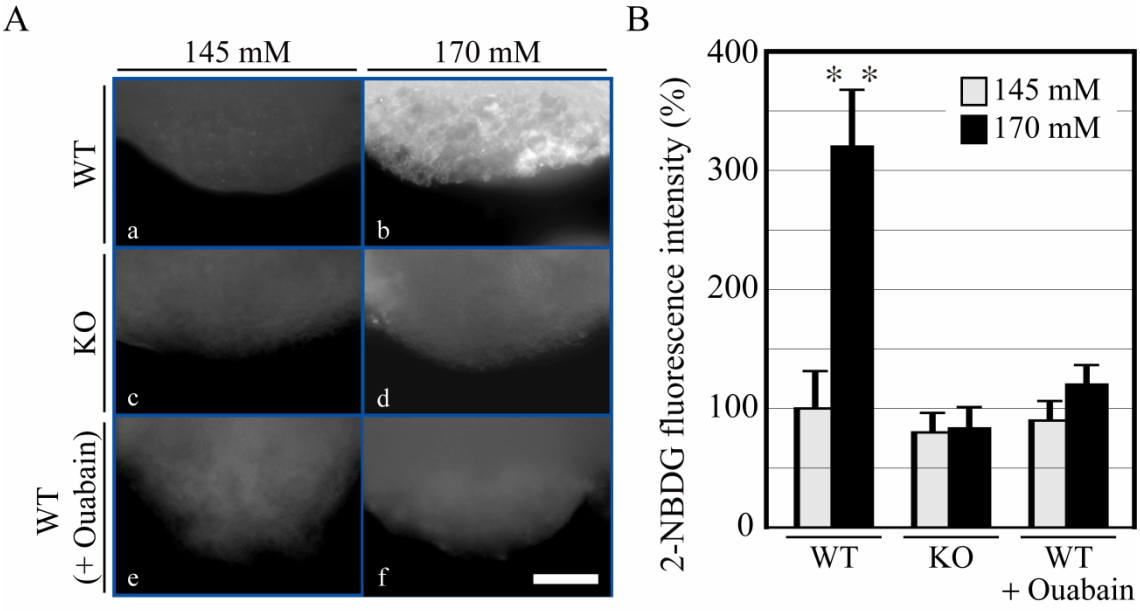

Fig. IV.1. Na_x channel is involved in Na-sensitive uptake of glucose in the SFO.

(A) Imaging analysis of the uptake of glucose in the SFO using a fluorescent glucose derivative. The SFO was isolated from wild-type (WT; Aa, Ab, Ae, and Af) and *Na_x*-KO (KO; Ac and Ad) mice, and incubated with 2-NBDG in the 145 mM (Aa, Ac, and Ae) or 170 mM (Ab, Ad, and Af) Na solution. In some experiments, the extracellular solutions contained 1 mM ouabain (Ae and Af). The tissues did not show any significant autofluorescence before incubation with 2-NBDG (not shown). Scale bar: 50 μm.

(B) Summary of glucose uptake activity of the SFO. Fluorescence intensities of the tissues were quantified by imaging software and the mean and SE was obtained. The mean fluorescence intensity of the wild-type in the 145 mM Na solution was set at 100%. **$p < 0.01$, two-tailed t test (against 145 mM of WT); data are the mean and SE ($n = 5$ for each).

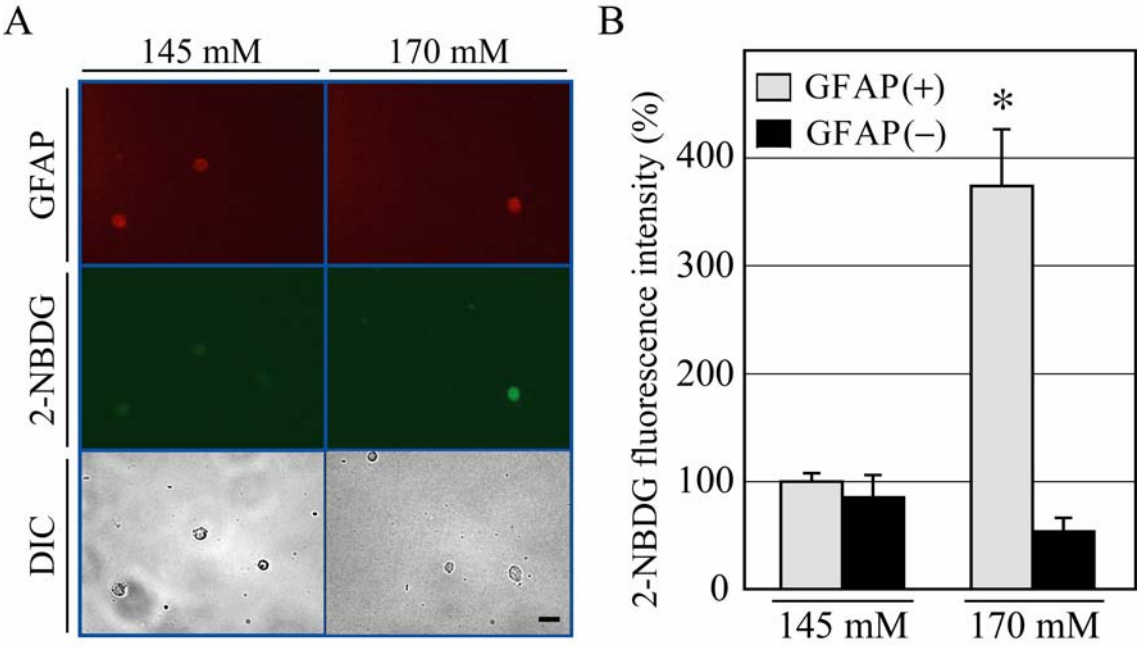

Fig. IV.2. Cells that intensively took up 2-NBDG are glial cells in SFO.

(A) Measurement of glucose-uptake activity of the cells dissociated from the SFO of wild-type mice. After the imaging analysis of glucose uptake using 2-NBDG in the 145 mM or 170 mM Na solution, cells were stained with the antibody for anti-glial fibrillary acidic protein (GFAP) antibody. DIC, differential interference contrast image. Scale bar: 50 μm.

(B) The summary of glucose-imaging studies in (A). GFAP (+), GFAP-immunopositive cells; GFAP (–), GFAP-immunonegative cells. *$p < 0.05$, Bonferroni's multiple comparison test (against GFAP (+) of 145 mM); data are the mean and SE (n = 15, each).

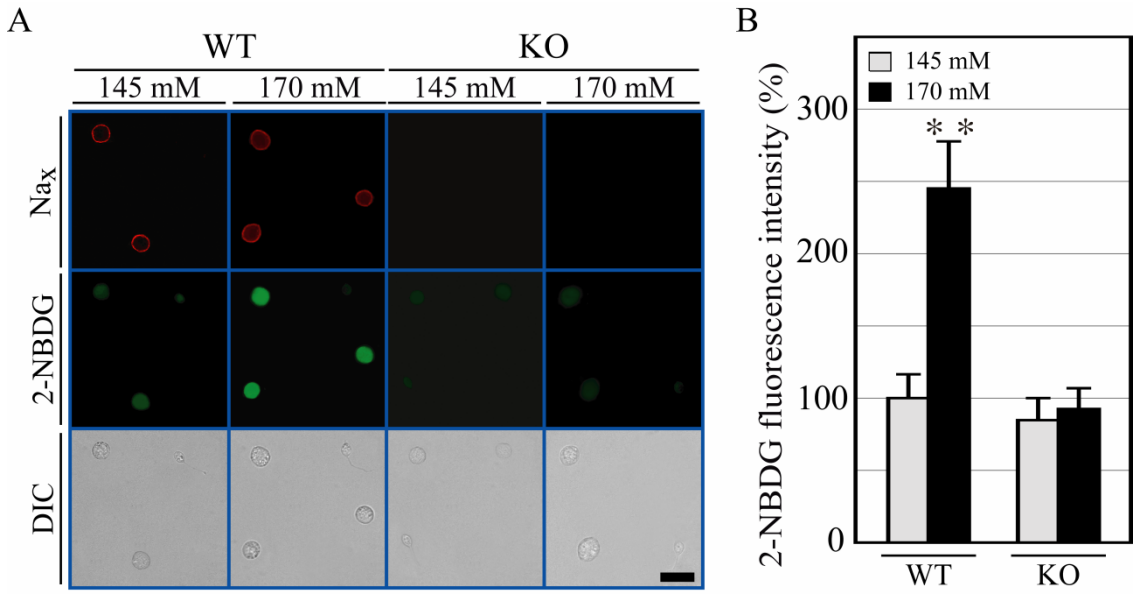

Fig. IV.3. Imaging analysis of glucose uptake in dissociated SFO cells.

(A) Cells dissociated from the SFO isolated from wild-type (WT) and *Na_x*-KO (KO) mice were subjected to imaging analysis of glucose uptake using 2-NBDG in the 145 mM or 170 mM Na solution. After the imaging, cells were stained with anti-Na_x channel antibody (Na_x). DIC, differential interference contrast image. Scale bar: 50 μm.

(B) Summary of glucose uptake activity of the SFO. The mean fluorescence intensity of *Na_x*-KO in the 145 mM solution was set at 100%. **p < 0.01, two-tailed t test (against 170 mM of KO); data are the mean and SE (n = 20 for each).

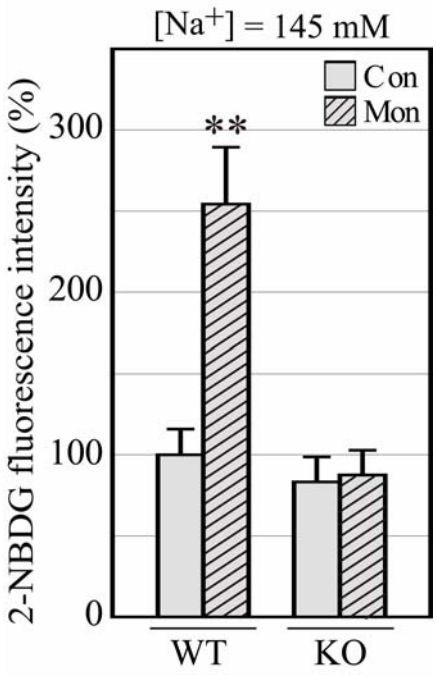

Fig. IV.4. Effect of monensin on glucose uptake in dissociated SFO cells.

Cells were dissociated from the SFO of wild-type (WT) and Na_x-KO (KO) mice. Cells were treated with 0.5 μM monensin (Mon) in the 145 mM Na solution. The mean fluorescence intensity of Con (without Mon treatment) of WT was set at 100%. **$p < 0.01$, two-tailed t test (against Con of WT); data are the mean and SE (n = 20 for each).

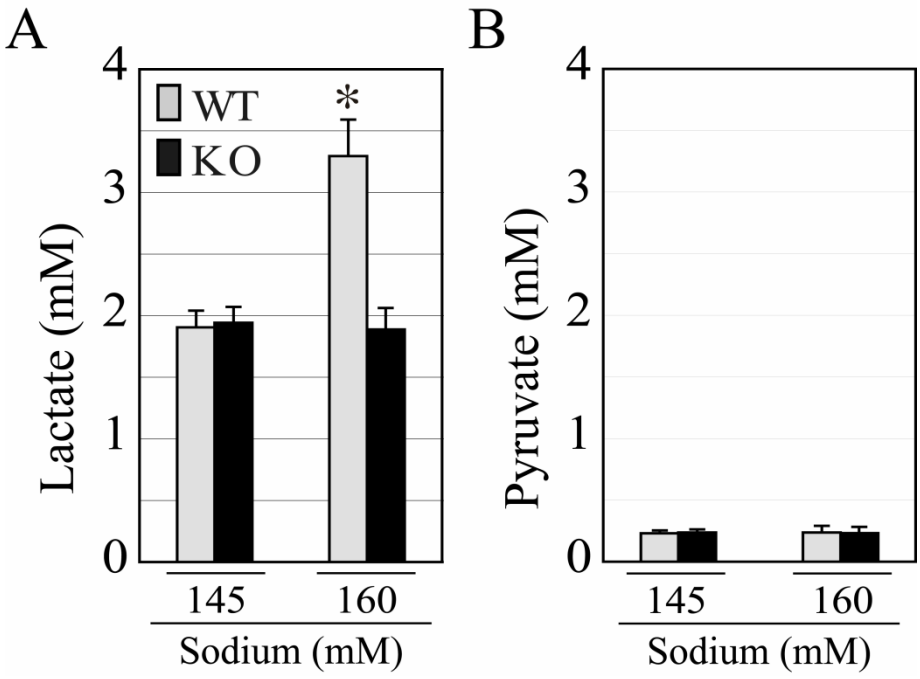

Fig. IV.5. Release of lactate and pyruvate from the SFO tissue into the incubation medium.

(A and B) Release of lactate (A) and pyruvate (B) from the SFO tissue into the incubation medium. Modified Ringer solutions, in which the SFO tissues from wild-type (WT) or Na_x-KO (KO) mice were incubated for 24 hr at 37˚C, were subjected to measurements by the enzyme assay. The normal modified Ringer solution and high Na modified Ringer solution contained 145 mM and 160 mM Na, respectively. *$p < 0.05$, two-tailed t test (against WT of 145 mM). Data are the mean and SE (n = 10 for each).

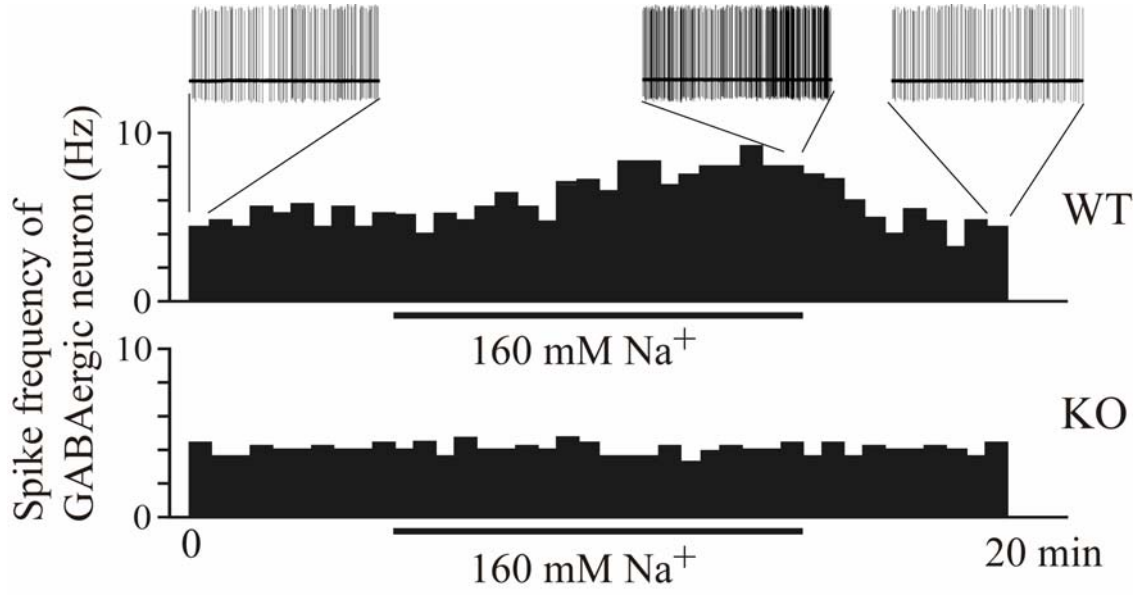

Fig. IV.6. Control of spike frequency of GABAergic neurons in the SFO by Na.
The SFO tissues from wild-type (WT) and *Na$_x$*-KO (KO) mice were treated with the high-Na modified Ringer solution. Na_x is indispensable for Na-dependent activation of the GABAergic neurons in the SFO.

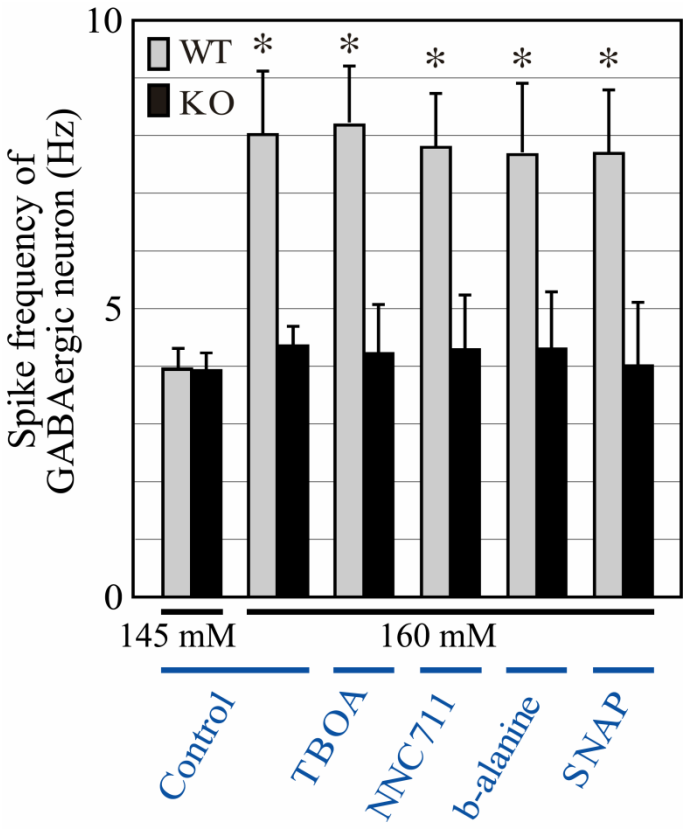

Fig. IV.7. Transporters for neurotransmitters are not involved in the Na-dependent enhancement of neuronal activities.

Electrophysiological experiments were performed with SFO slices of wild-type (WT) and Na_x-KO (KO) mice. Means of the spike frequency of GABAergic neurons during the perfusion of various kinds of solutions are shown. TBOA, 100 μM TBOA (an inhibitor for EAAT3); NNC711, 0.1 μM NNC711, (a specific inhibitor for GAT1); β-alanine, 100 μM β-alanine (a specific inhibitor for GAT1/2); SNAP, 25 μM SNAP-5114 (a specific inhibitor for GAT2/3). *$p < 0.05$, Bonferroni's multiple comparison test (against WT of Control in 145 mM); data are the mean and SE (n = 4, each).

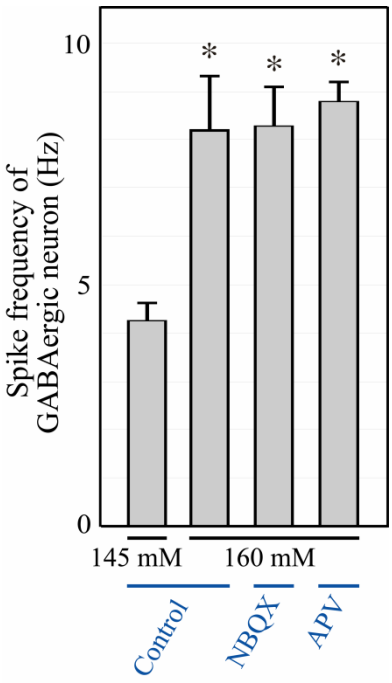

Fig. IV.8. Glutamatergic transmission is not involved in the Na-dependent enhancement of neuronal activities.

Electrophysiological experiments were performed with SFO slices of wild-type mice. Means of the spike frequency of GABAergic neurons during the perfusion with various solutions are shown. NBQX, 25 μM NBQX (an antagonist for AMPA/Kainate receptors); APV, 50 μM D-APV (an antagonist for NMDA receptor). *$p < 0.05$, Bonferroni's multiple comparison test (against WT of Control in 145 mM); data are the mean and SE (n = 4, each).

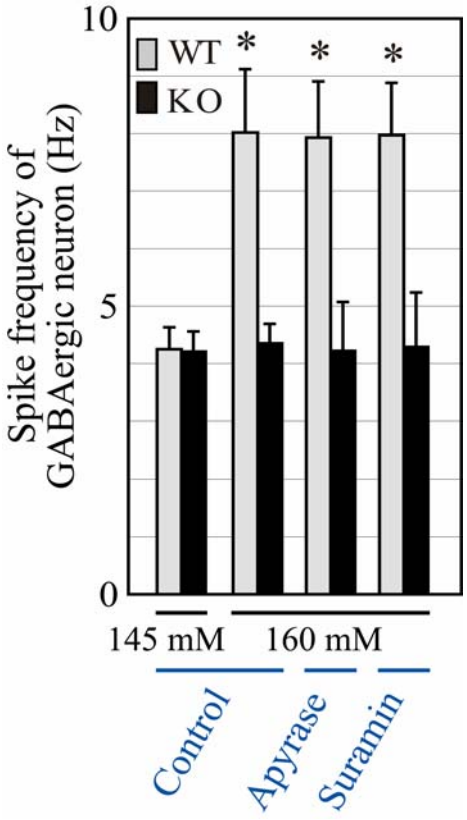

Fig. IV.9. Purinergic signaling is not involved in the Na-dependent enhancement of neuronal activities.

Electrophysiological experiments with SFO slices of wild-type (WT) and Na_x-KO (KO) mice. Means of the spike frequency of GABAergic neurons during the perfusion of various kinds of solutions are shown. Apyrase, 1 unit/ml apyrase (an ATPase); Suramin, 30 μM suramin (an antagonist for P2 purinergic receptors). *$p < 0.05$, Bonferroni's multiple comparison test (against WT of Control in 145 mM); data are the mean and SE (n = 4, each).

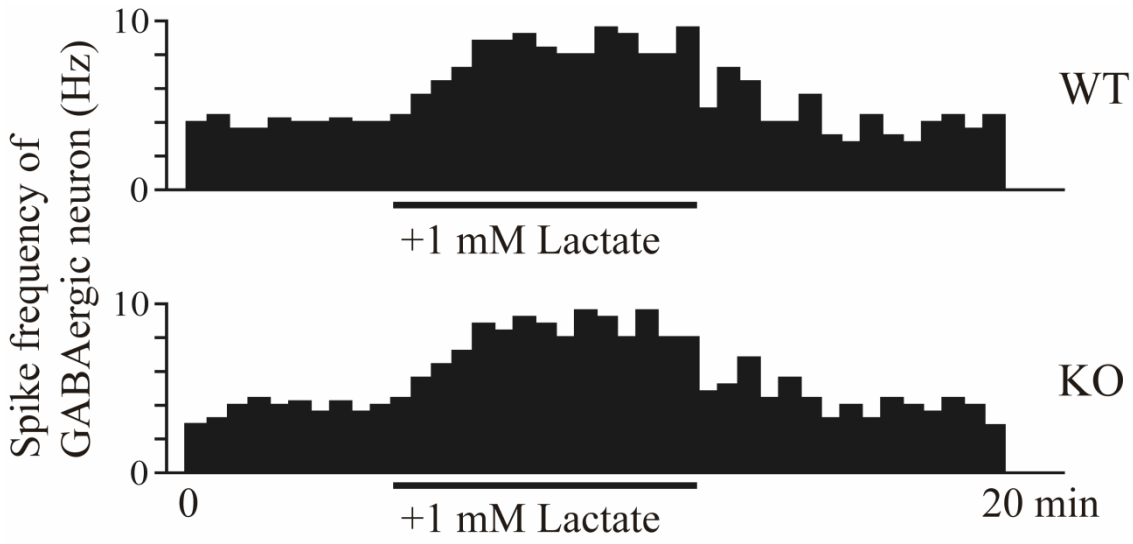

Fig. IV.10. Control of spike frequency of GABAergic neurons in the SFO by lactate.

The SFO tissues from wild-type (WT) and *Na*$_x$-KO (KO) mice were treated with 1 mM lactate in the normal modified Ringer solution. Lactate activates the GABAergic neurons independent of Na_x.

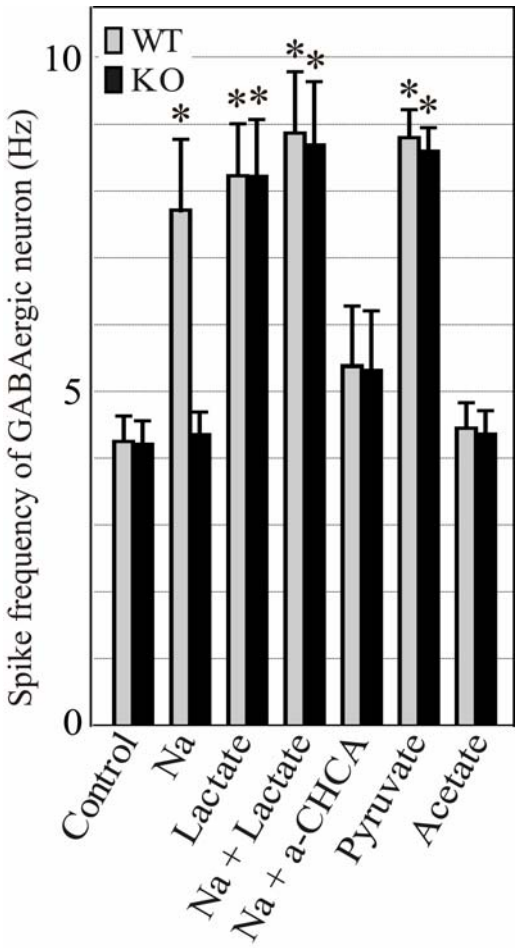

Fig. IV.11. Summary of the electrophysiological experiments with the SFO of wild-type (WT) and Na_x-KO (KO) mice.

Means of spike frequency of the GABAergic neurons during perfusion of various kinds of solutions are shown. Na, 160 mM Na solution; Lactate, 1 mM lactate; α-CHCA, 5 mM α-Cyano-4-hydroxycinnamic acid (an inhibitor of monocarboxylate transporters); Pyruvate, 1 mM pyruvate; Acetate, 1 mM acetate; *$p < 0.05$, Bonferroni's multiple comparison test (against WT of control). Data are the mean and SE (n = 8 for each).

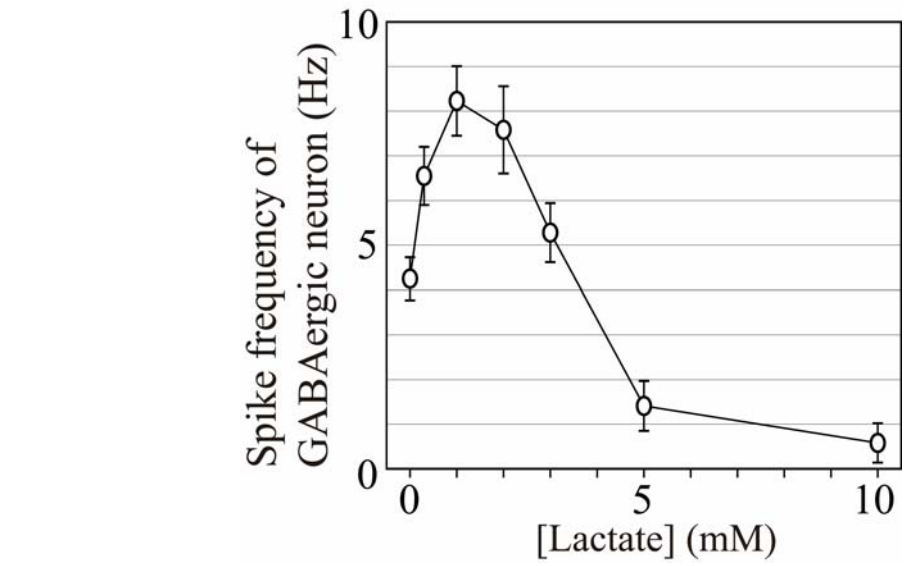

Fig. IV.12. Concentration dependency of lactate's effect on of the spike frequency of GABAergic neurons.

The SFO tissues of wild-type mice were used for this experiment. Data are the mean and SE (n = 5 for each).

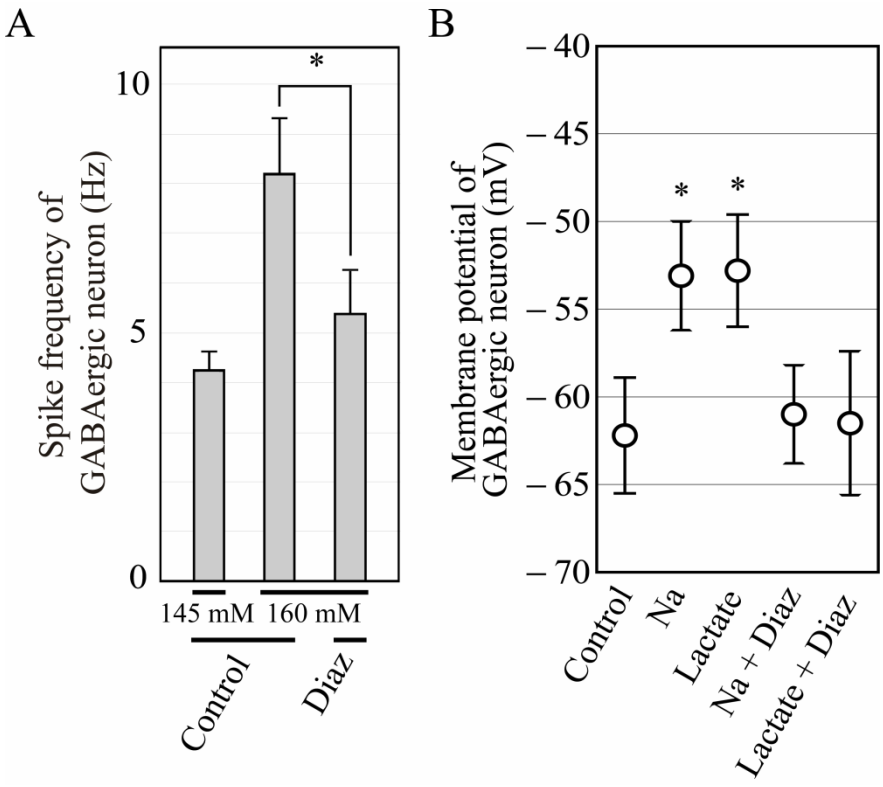

Fig. IV.13. Putative role of K_{ATP} channel in Na-dependent stimulation of GABAergic neurons in the SFO.

Electrophysiological experiments were performed with SFO slices of wild-type mice. (A) Means of the spike frequency of GABAergic neurons during the perfusion with various kinds of solutions are shown. Diaz, 0.3 mM diazoxide, an opener of K_{ATP} channel. *$p < 0.05$, two-tailed t test (against Control of 160 mM); data are the mean and SE (n = 5 for each).

(B) The membrane potentials of GABAergic neurons in the presence of 1 μM TTX. Na, 160 mM Na solution; Lactate, 1 mM lactate; Diaz, 0.3 mM diazoxide; *$p < 0.05$, Bonferroni's multiple comparison test (against Control); data are the mean and SE (n = 20 for each).

Chapter V

Summary and conclusion

In this thesis, I revealed the signaling mechanism from glial cells to neurons underling the Na-sensing mechanism in the SFO. The Na_x channel is a Na-level-sensitive Na channel which opens in response to an increase of the Na concentration in the extracellular fluid in the physiological range (Hiyama *et al*., 2002). Increases in Na level in body fluids are sensed by Na_x in specific glial cells in the sensory CVOs (Watanabe *et al*., 2006). Among the CVOs, the SFO appears to be the center of the sensing responsible for the control of Na-intake behavior (Hiyama *et al*., 2004). A recent report from our laboratory showed that Na_x channels populate the cellular processes of astrocytes and ependymal cells enveloping neurons including GABAergic neurons in the SFO (Watanabe *et al*., 2006).

In the present study, I showed that there exists direct interaction between Na_x and α subunits of Na^+/K^+-ATPase, which enables the Na_x-positive glial cells to Na-dependently activate the anaerobic metabolism of glucose. Na-level-dependent Na^+ influx through Na_x and direct interaction between Na_x and Na^+/K^+-ATPase are the basis for activation of Na^+/K^+-ATPase in the glial cells. Activation of Na^+/K^+-ATPase stimulates anaerobic metabolism of glucose by the glial cells, which produces lactate as the end product. Na-dependent lactate production was specifically observed in the SFO of wild-type mice, but not of *Na_x*-KO mice. There exist GABAergic neurons spontaneously firing in the SFO. Lactate released from the glial cells functions as the substance signaling to the neurons for activation. Lactate released from Na_x-positive glial cells thus appears to be a neurostimulator in the SFO to control the Na-intake behavior.

The schematic summary of these cellular mechanisms are illustrated in a picture (Fig. V.1). The sensory CVOs, including the SFO, are characterized by the presence of the neuronal cell bodies and extensive networks of fenestrated capillaries which allow ingredients of plasma to release to the intercellular space. Their ventricular side is partitioned by an ependymal cell layer facing to the third ventricle. Na_x channels populate perineural processes of astrocytes and ependymal cells in the SFO (Watanabe *et al*., 2006). When animals are dehydrated, Na concentration in plasma and CSF increases above the usual level of ~145 mM ((1) in Fig. V.1). When the extracellular

Na concentration exceeds ~150 mM, Na_x channels open, and the intracellular Na concentration in these glial cells is increased. This leads to activation of Na^+/K^+-ATPase in these cells ((2) in Fig. V.1). Activated Na^+/K^+-ATPase consumes ATP larger than the usual level to pump out Na ions ((3) in Fig. V.1). To fuel Na^+/K^+-ATPase with ATP, the glial cells enhance the glucose uptake to stimulate the anaerobic glycolysis ((4) in Fig. V.1). Lactate, the end product of the anaerobic glycolysis, is released from the glial cells and supplied to neurons, including GABAergic neurons, through the processes enveloping them ((5) in Fig. V.1). Lactate stimulates the activity of the GABAergic neurons through production of ATP, which presumably regulate hypothetic neurons involved in the control of salt-intake behavior ((6) in Fig. V.1). In dehydrated KO mice, the Na-dependent stimulation of glycolysis is impaired and the activity of the GABAergic neurons is not promoted. This figure shows the case of ependymal cells, however, the same scheme would be applicable for Na_x-positive astrocytes.

In conclusion, lactate is the signaling substance that is controlled by glial Na_x channels and transmitted from the glial cells to neurons for Na-sensing in the brain. To my knowledge, this study is the first to show that glial cells take the initiative in the regulation of neural activity using lactate as a signaling substance.

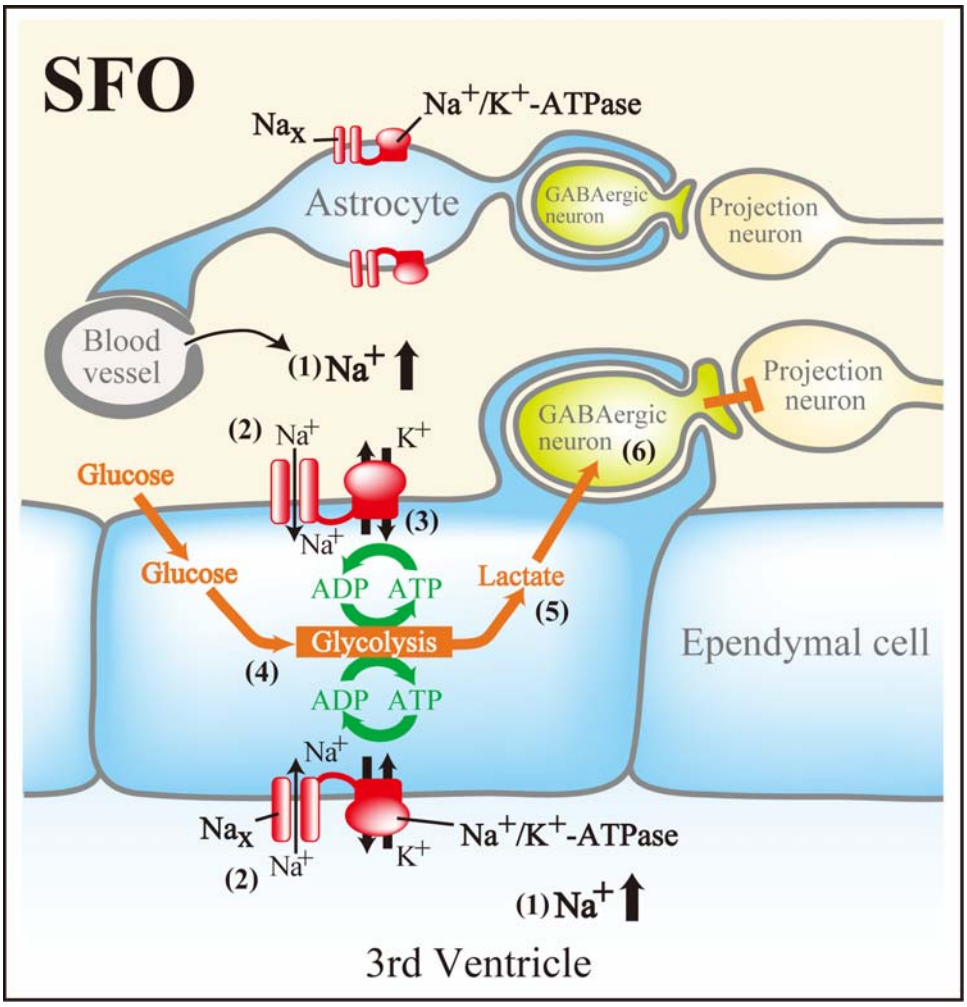

Fig. V.1. Schematic overview of the Na-level sensing mechanism and Na-dependent regulation of neurons in the SFO.

When animals are dehydrated, Na concentration in plasma and CSF increases above the usual level of ~145 mM (1). When the extracellular Na concentration exceeds ~150 mM, Na_x channels open, and the intracellular Na concentration in these glial cells is increased. This leads to activation of Na^+/K^+-ATPase in these cells (2). Activated Na^+/K^+-ATPase consumes ATP larger than the usual level to pump out Na ions (3). To fuel Na^+/K^+-ATPase with ATP, the glial cells enhance the glucose uptake to stimulate the anaerobic glycolysis (4). Lactate, the end product of the anaerobic glycolysis, is released from the glial cells and supplied to neurons, including GABAergic neurons, through the processes enveloping them (5). Lactate stimulates the activity of the

GABAergic neurons through production of ATP, which presumably regulate hypothetic neurons involved in the control of salt-intake behavior (6). In dehydrated KO mice, the Na-dependent stimulation of glycolysis is impaired and the activity of the GABAergic neurons is not promoted. This figure shows the case of ependymal cells, however, the same scheme would be applicable for Na_x-positive astrocytes.

Chapter VI

References

Akopian, A.N., Souslova, V., Sivilotti, L., and Wood, J.N. (1997). Structure and distribution of a broadly expressed atypical sodium channel. FEBS Lett. *400*, 183–187

Andersson, B. (1978). Regulation of water intake. Physiol. Rev. *58*, 582–603.

Anderson, C.M., and Swanson, R.A. (2000). Astrocyte glutamate transport: review of properties, regulation, and physiological functions. Glia *32*, 1–14.

Asanuma, K., Ariga, T., Aida, N., Miyasaka, A., Nagai, Y., Miyagawa, T., Minowa, M., Yoshida, M., Tsuda, M., and Tatano, T. (1985). A new method for simultaneous autoanalysis of plasma levels of lactic acid and pyruvic acid by means of the oxidase system. Anal. Clin. Specimen (in Japanese) *8*, 16–24.

Bartel, P.L., and Fields, S. (1995). Analyzing protein-protein interactions using two-hybrid system. Methods Enzymol. *254*, 241–263.

Boer, P.H., Potten, H., Adra, C.N., Jardine, K., Mullhofer, G., and McBurney, M.W. (1990). Polymorphisms in the coding and noncoding regions of murine Pgk-1 alleles. Biochem. Genet. *28*, 299–308.

Chae, H.E., and Heideman, P.D. (1998). Water-deprived white-footed mice express c-*fos* on a day/night cycle graded according to the duration of deprivation. Brain Res., *791*, 1–10

Chih, C.P., Lipton, P., and Roberts, E.L. Jr. (2001). Do active cerebral neurons really use lactate rather than glucose? Trends Neurosci. *24*, 573–578.

Conti, F., Minelli, A., and Melone, M. (2004). GABA transporters in the mammalian cerebral cortex: localization, development and pathological implications. Brain Res. Brain Res. Rev. *45*, 196–212.

Cox, P.S., Denton, D.A., Mouw, D.R., and Tarjan, E. (1987). Natriuresis induced by

localized perfusion within the third cerebral ventricle of sheep. Am. J. Physiol. Regul. Integr. Comp. Physiol. *252*, R1–6.

Denton, D.A., McKinley, M.J., and Weisinger, R.S. (1996). Hypothalamic integration of body fluid regulation. Proc. Natl. Acad. Sci. USA *93*, 7397–7404.

Felipe, A., Knittle, T.J., Doyle K.L., and Tamkun, M.M. (1994). Primary structure and differential expression during development and pregnancy of a novel voltage-gated sodium channel in the mouse. J. Biol. Chem. *269*, 30125–30131

Feschenko, M.S., Donnet, C., Wetzel, R.K., Asinovski, N.K., Jones, L.R., Sweadner, K.J. (2003). Phospholemman, a single-span membrane protein, is an accessory protein of Na,K-ATPase in cerebellum and choroid plexus. J. Neurosci. *23*, 2161–2169.

Fields, R.D., and Burnstock, G. (2006). Purinergic signalling in neuron-glia interactions. Nat. Rev. Neurosci. *7*, 423–436.

Fujikawa, A., Shirasaka, D., Yamamoto, S., Ota, H., Yahiro, K., Fukada, M., Shintani, T., Wada, A., Aoyama, N., Hirayama, T., Fukamachi, H., Noda, M. (2003). Mice deficient in protein tyrosine phosphatase receptor type Z are resistant to gastric ulcer induction by VacA of Helicobacter pylori. Nat. Genet. *33*, 375–381.

Garty, H., Lindzen, M., Scanzano, R., Aizman, R., Fuzesi, M., Goldshleger, R., Farman, N., Blostein, R., and Karlish, S.J. (2002). A functional interaction between CHIF and Na^+/K^+-ATPase: implication for regulation by FXYD proteins. Am. J. Physiol. Renal. Physiol. *283*, F607–615.

Gautron, S., Dos Santos, G., Pinto-Henrique, D., Koulakoff, A., Gros, F., and Berwald-Netter, Y. (1992). The glial voltage-gated Na channel: cell- and tissue-specific mRNA expression. Proc. Natl. Acad. Sci. USA *89*, 7272–7276.

George, A.L.J., Knittle, T.J., and Tamkun, M.M. (1992). Molecular Cloning of an

Atypical Voltage-Gated Sodium Channel Expressed in Human Heart and Uterus: Evidence for a Distinct Gene Family. Proc. Natl. Acad. Sci. USA *89*, 4893–4897

Gladden, L.B. (2004). Lactate metabolism: a new paradigm for the third millennium. J. Physiol. *558*, 5–30.

Goldberg, J.A., and Wilson, C.J. (2005). Control of spontaneous firing patterns by the selective coupling of calcium currents to calcium-activated potassium currents in striatal cholinergic interneurons. J. Neurosci. *25*, 10230–10238.

Goldin, A.L., Barchi, R.L., Caldwell, J.H., Hofmann, F., Howe, J.R., Hunter, J.C., Kallen, R.G., Mandel, G., Meisler, M.H., Netter, Y.B., Noda, M., Tamkun, M.M., Waxman, S.G., Wood, J.N., and Catterall, W.A. (2000). Nomenclature of voltage-gated Na channels. Neuron *28*, 365–368.

Harootunian, A.T., Kao, J.P., Eckert, B.K., and Tsien, R.Y. (1989). Fluorescence ratio imaging of cytosolic free Na^+ in individual fibroblasts and lymphocytes. J. Biol. Chem. *264*, 19458–19467.

Hertz, L., and Dienel, G.A. (2004). Lactate transport and transporters: general principles and functional roles in brain cells. J. Neurosci. Res. *79*, 11–18.

Hiyama, T.Y., Watanabe, E., Okado, H., and Noda, M. (2004). The subfornical organ is the primary locus of Na-level sensing by Na_x Na channels for the control of salt-intake behavior. J. Neurosci. *24*, 9276–9281.

Hiyama, T.Y., Watanabe, E., Ono, K., Inenaga, K., Tamkun, M.M., Yoshida, S., and Noda, M. (2002). Na_x channel involved in CNS Na-level sensing. Nat. Neurosci. *5*, 511–512.

Hu, Y., and Wilson G.S. (1997). A temporary local energy pool coupled to neuronal activity: fluctuations of extracellular lactate levels in rat brain monitored with

rapid-response enzyme-based sensor. J. Neurochem. *69*, 1484–1490.

Hyder, F., Patel, A.B., Gjedde, A., Rothman, D.L., Behar, K.L., and Shulman, R.G. (2006). Neuronal-glial glucose oxidation and glutamatergic-GABAergic function. J. Cereb. Blood Flow Metab. *26*, 865–877.

Jewell, E.A., and Lingrel, J.B. (1991). Comparison of the substrate dependence properties of the rat Na^+/K^+-ATPase alpha 1, alpha 2, and alpha 3 isoforms expressed in HeLa cells. J. Biol. Chem. *266*, 16925–16930.

Johnson, A.K., and Gross, P.M. (1993). Sensory circumventricular organs and brain homeostatic pathways. FASEB J. *7*, 678–686.

Johnson, R.F., Beltz, T.G., Thunhorst, R.L., and Johnson, A.K. (2003). Investigations on the physiological controls of water and saline intake in C57BL/6 mice. Am. J. Physiol. Regul. Integr. Comp. Physiol. *285*, R294–R403

Jung, J., Yoon, T., Choi, E.C., Lee, K. (2002). Interaction of cofilin with triose-phosphate isomerase contributes glycolytic fuel for Na,K-ATPase via Rho-mediated signaling pathway. J Biol Chem. *277*, 48931–48937.

Kaplan, J.H. (2002). Biochemistry of Na,K-ATPase. Ann. Rev. Biochem. *71*, 511–535.

Kondo, S., and Marty, A. (1998). Differential effects of noradrenaline on evoked, spontaneous and miniature IPSCs in rat cerebellar stellate cells. J. Physiol. *509*, 233–243.

Krivoi, I.I., Drabkina, T.M., Kravtsova, V.V., Vasiliev, A.N., Eaton, M.J., Skatchkov, S.N., Mandel, F. (2006). On the functional interaction between nicotinic acetylcholine receptor and Na^+,K^+-ATPase. Pflugers Arch. *452*, 756–765.

Maeda N, Hamanaka H, Shintani T, Nishiwaki T, and Noda M (1994). Multiple receptor-like protein tyrosine phosphatases in the form of chondroitin sulfate proteoglycan. FEBS Lett. *354*, 67–70.

Magistretti, P.J. (2000). Cellular bases of functional brain imaging: insights from neuron-glia metabolic coupling. Brain Res. *886*, 108–112.

Masson, J., Sagne, C., Hamon, M., and El Mestikawy, S. (1999). Neurotransmitter transporters in the central nervous system. Pharmacol. Rev. *51*, 439–464.

McGrail, K.M., Phillips, J.M., and Sweadner, K.J. (1991). Immunofluorescent localization of three Na,K-ATPase isozymes in the rat central nervous system: both neurons and glia can express more than one Na,K-ATPase. J. Neurosci. *11*, 381–391.

McKinley, M.J., McAllen, R.M., Davern, P., Giles, M.E., Penschow, J., Sunn, N., Uschakov, A., and Oldfield, B.J. (2003). The sensory circumventricular organs of the mammalian brain. Adv. Anat. Embryol. Cell Biol. *172*, III-XII, 1–122.

Morien, A., Garrard, L., and Rowland, N.E. (1999). Expression of Fos immunoreactivity in rat brain during dehydration: effect of duration and timing of water deprivation. Brain Res. *816*, 1–7

Noda, M. (2006). The subfornical organ, a specialized Na channel, and the sensing of Na levels in the brain. Neuroscientist *12*, 80–91.

Noda, M., and Hiyama, T.Y. (2005). Na-level-sensitive Na channel and salt-intake behavior. Chem. Senses *30*, i44–45.

Nose H., Doi Y., Usui S., Kubota T., Fujimoto M., and Morimoto T. (1992). Continuous measurement of Na concentration in CSF during gastric water infusion in dehydrated rats. J. Appl. Physiol. *73*, 1419 –1424.

Park, R., Denton, D.A., McKinley, M.J., Pennington, G., and Weisinger, R.S. (1989). Intracerebroventricular saccharide infusions inhibit thirst induced by systemic hypertonicity. Brain Res. *493*, 123–128.

Pellerin, L., Pellegri, G., Bittar, P.G., Charnay, Y., Bouras, C., Martin, J.L., Stella, N., and Magistretti, P.J. (1998). Evidence supporting the existence of an activity-dependent astrocyte-neuron lactate shuttle. Dev. Neurosci. *20*, 291–299.

Rosenthal, M., and Sick, T.J. (1992). Glycolytic and oxidative metabolic contributions to potassium ion transport in rat cerebral cortex. Can. J. Physiol. Pharmacol. *70 Suppl*, S165–169.

Serpersu, E.H., and Tsong, T.Y. (1984). Activation of electrogenic Rb^+ transport of (Na,K)-ATPase by an electric field. J. Biol. Chem. *259*, 7155–7162.

Shamraj, O.I., and Lingrel, J.B. (1994). A putative fourth Na^+,K^+-ATPase alpha-subunit gene is expressed in testis. Proc. Natl. Acad. Sci. USA *91*, 12952–12956.

Sibson, N.R., Dhankhar, A., Mason, G.F., Rothman, D.L., Behar, K.L., and Shulman, R.G. (1998). Stoichiometric coupling of brain glucose metabolism and glutamatergic neuronal activity. Proc. Natl. Acad. Sci. USA *95*, 316–321.

Song, Z., and Routh, V.H. (2005). Differential effects of glucose and lactate on glucosensing neurons in the ventromedial hypothalamic nucleus. Diabetes *54*, 15–22.

Sweadner, K.J. (1989). Isozymes of the Na^+/K^+-ATPase. Biochim. Biophys. Acta *988*, 185–220

Sweadner, K.J. (1995). Na, K-ATPase and its isoforms. In: *Neuroglia*, edited by Kettenmann, H., and Ransom, B.R. Oxford University Press, New York, 259–272

Ueta, Y., Yamashita, H., Kawata, M., and Koizumi, K. (1995). Water deprivation

induces regional expression of c-*fos* protein in the brain of inbred polydipsic mice. *677*, 221–228

Vojtek, A.B., and Hollenberg, S.M. (1995). Ras-Raf interaction: two-hybrid analysis. Methods Enzymol. *255*, 331–342.

Vojtek, A.B., Hollenberg, S.M., and Cooper, J.A. (1993). Mammalian Ras interacts directly with the serine/threonine kinase Raf. Cell *74*, 205–214.

Wakerley J.B., Poulain D.A., and BrownD (1978) Comparison of firing patterns in oxytocin- and vasopressin-releasing neurones during progressive dehydration. Brain Res. *148*, 425– 440.

Wang, X.Q., Yu, S.P. (2005). Novel regulation of Na, K-ATPase by Src tyrosine kinases in cortical neurons. J. Neurochem. *93*, 1515–1523.

Waniewski, R.A., and Martin, D.L., (2004). Astrocytes and synaptosomes transport and metabolize lactate and acetate differently. Neurochem. Res. *29*, 209–217.

Washburn, D.L., Anderson, J.W., and Ferguson, A.V. (2000). A subthreshold persistent Na current mediates bursting in rat subfornical organ neurones. J. Physiol. *529 Pt 2*, 359–371.

Watanabe, E., Fujikawa, A., Matsunaga, H., Yasoshima, Y., Sako, N., Yamamoto, T., Saegusa, C., and Noda, M. (2000). Na_v2/NaG channel is involved in control of salt-intake behavior in the CNS. J. Neurosci. *20*, 7743–7751.

Watanabe, E., Hiyama, T.Y., Shimizu, H., Kodama, R., Hayashi, N., Miyata, S., Yanagawa, Y., Obata, K., and Noda, M. (2006). Na-level-sensitive Na channel Na_x is expressed in glial laminate processes in the sensory circumventricular organs. Am. J. Physiol. Regul. Integr. Comp. Physiol. *290*, R568–R576.

Watts, A.G., Sanchez-Watts, G., Emanuel, J.R., and Levenson, R. (1991). Cell-specific expression of mRNAs encoding Na^+,K^+-ATPase alpha- and beta-subunit isoforms within the rat central nervous system. Proc. Natl. Acad. Sci. USA *88*, 7425–7429.

Weisinger, R.S., Considine, P., Denton, D.A., and McKinley, M.J. (1979). Rapid effect of change in cerebrospinal fluid Na concentration on salt appetite. Nature *280*, 490–491.

Yamada, K., Nakata, M., Horimoto, N., Saito, M., Matsuoka, H., and Inagaki, N. (2000). Measurement of glucose uptake and intracellular calcium concentration in single, living pancreatic beta-cells. J. Biol. Chem. *275*, 22278–22283.

Yoshioka, K., Takahashi, H., Homma, T., Saito, M., Oh, K. B., Nemoto, Y., and Matsuoka, H. (1996). A novel fluorescent derivative of glucose applicable to the assessment of glucose uptake activity of Escherichia coli. Biochim. Biophys. Acta *1289*, 5–9.

Zouzoulas, A., Blostein, R. (2006). Regions of the catalytic alpha subunit of Na,K-ATPase important for functional interactions with FXYD 2. J. Biol. Chem. *281* 8539–8544.

Acknowledgements

I wish to thank Prof. Masaharu Noda for guidance and support especially the passing on of a wealth of scientific knowledge and experience. I wish to thank Dr. Eiji Watanabe, Dr. Takeshi Y. Hiyama and Dr. Akihiro Fujikawa for their support in some experiments; especially establishment of cell lines, imaging and electrophysiological analysis, and biochemical analysis, respectively. I wish to thank all the current and past members of the lab for helpful advice.